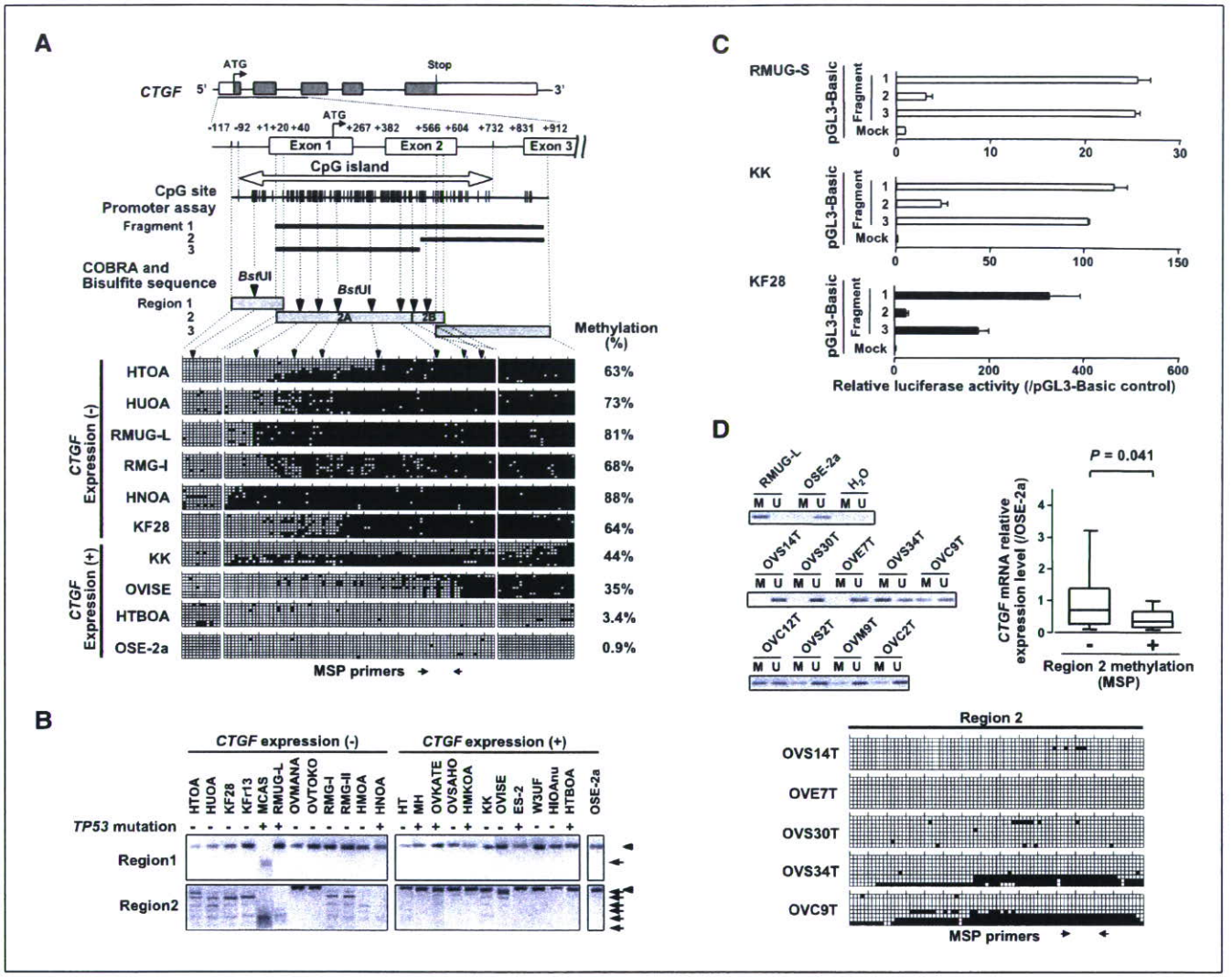

Figure 2. Methylation status of the *CTGF* CpG-rich region in ovarian cancer cell lines. *A*, schematic map of the CpG-rich region containing the CpG island (*closed white arrow*) around exon 1 of *CTGF* and representative results of bisulfite sequencing. CpG sites (*vertical ticks on the expanded axis*). Exons (*open box*). The transcription-start site is marked at +1. The fragments examined in a promoter assay (*thick black lines*). The regions examined in the COBRA and bisulfite sequencing (*horizontal gray bars*). Restriction sites for *Bst*UI (for the COBRA; *black downward arrowheads*). Representative results of bisulfite sequencing of the *CTGF* CpG-rich region examined in *CTGF*-expressing ovarian cancer cell lines (+) and *CTGF*-nonexpressing ovarian cancer cell lines (−). Each square indicates a CpG site: *open squares*, unmethylated; *solid squares*, methylated. PCR primers for MSP (*arrows*). *B*, representative results of the COBRA of the *CTGF* CpG island in ovarian cancer cell lines after restriction with *Bst*UI. *Arrows*, fragments specifically restricted at sites recognized as methylated CpGs; *arrowheads*, undigested fragments indicating unmethylated CpGs. *C*, promoter activity of the *CTGF* CpG-rich region. pGL3-Basic empty vectors (mock) and constructs containing one of three different sequences around the highly methylated region of *CTGF* (fragments 1–3 with a 157, 584, and 346 bp size, respectively, in *A*) were transfected into RMUG-S, KK, and KF28 cells. Luciferase activity was normalized versus an internal control. *Columns*, mean of three separate experiments, each done in triplicate; *bars*, SD. *D*, *top left*, representative results of a MSP analysis of the *CTGF* promoter region in primary ovarian cancer tissues. Parallel amplification reactions were done using primers specific for unmethylated (*U*) or methylated (*M*) DNA. *Top right*, correlation between methylation status of *CTGF* determined by MSP and mRNA expression status determined by RT-PCR in 43 primary tumors except for mucinous type tumors. Statistical analysis used the Mann-Whitney *U* test. *Horizontal bars in the boxes*, median values; *vertical bars*, range; *horizontal boundaries of the boxes*, first and third quartiles. *Bottom*, methylation status of the *CTGF* promoter region determined by bisulfite sequencing in tumor samples. *Arrows*, the positions of primers for MSP.

CTGF protein expression was not clearly associated with the methylation status of *CTGF* region 2, even in tumors other than mucinous type tumors (P = 0.215, Fisher's exact test; data not shown). CTGF protein expression was significantly associated with tumor stage: ovarian cancer tended to lack CTGF expression in the earlier stages (stages I and II) but tended to exhibit CTGF expression in the advanced stages (stages III and IV; P = 0.027, χ^2 test). CTGF protein was also differentially expressed among histologic subtypes. However, no significant relationship was found between the level of CTGF expression and the age of patients, the result of surgery, or the result of peritoneal cytology. In overall survival, no significant difference was observed between the patients with lower levels of CTGF and those with higher levels of CTGF in all stages and in stage III and IV disease (P = 0.158 and 0.148, respectively, log-rank test; data not shown). In stage I and II disease, however, no deaths occurred in patients with higher levels of CTGF expression during the study period, whereas 17.5% (10 of 57 cases) of patients with lower levels of expression died, although a statistical analysis could not be done due to no deaths in one group (Fig. 3*D*). Those findings suggest

that the incidence of the inactivation of CTGF and its role in tumorigenesis may differ with the stage and/or histologic subtype of this disease.

Suppression of cell growth induced by CTGF in ovarian cancer cells. The frequent silencing of *CTGF* in cell lines and primary tumors of ovarian cancer suggests that CTGF is likely to be a functional tumor suppressor for this disease. To investigate whether restoration of CTGF expression would suppress growth of ovarian cancer cells in which the gene had been silenced, we did colony formation assays using an expression construct of the full-coding sequence of *CTGF* (Fig. 4*A*). Two weeks after transfection and subsequent selection of drug-resistant colonies, the numbers of larger colonies produced by *CTGF*-transfected cells decreased compared with those of cells containing empty vector, regardless of mutation status of the *TP53* gene (Fig. 2*B*).

To avoid a nonspecific toxicity by forced expression of CTGF, we assessed the effect of recombinant human CTGF on growth of the nonexpressing ovarian cancer cells (Fig. 4*B, top*). Treatment with recombinant CTGF for 72 h reduced cell viability in HNOA and HMOA cell lines compared with vehicle (PBS) alone. In FACS analysis using HMOA cell line (Fig. 4*B, bottom*), treatment with recombinant CTGF resulted in an accumulation of cells in G_0-G_1 phase and a decrease in S and G_2-M phase cells but no increase in sub-G_1 phase cells compared with vehicle alone, suggesting that CTGF may arrest ovarian cancer cells at the G_1-S checkpoint (G_0-G_1 arrest) without inducing apoptosis.

To further examine the mechanisms of CTGF-induced growth inhibition in ovarian cancer cells, we investigated the effect of CTGF on EGF-dependent phosphorylation of ERK1/2 in HMOA cell line because (*a*) the overexpression of the EGF receptor is associated with poor prognosis of ovarian cancer (31) and (*b*) the suppressive effect of CTGF overexpression on EGF-dependent phosphorylation has been reported in non–small cell lung cancer (NSCLC) cell line (16). In serum-starved HMOA cells, ERK1/2 was remarkably phosphorylated with EGF treatment and the level of phosphorylation was decreased by pretreatment with CTGF (Fig. 4*C*).

To confirm a growth-suppressive effect of CTGF, we knocked down endogenously expressed CTGF by transient transfection of *CTGF*-siRNA to KK and ES-2 cell lines retaining expression of CTGF (Fig. 4*D*). Transfection of *CTGF*-siRNA accelerated cell growth in those cell lines compared with *Luc*-siRNA–transfected counterparts. Because transfection of *CTGF*-siRNA to RMUG-S cell line lacking *CTGF* expression showed no effect on cell growth compared with *Luc*-siRNA, growth-promoting effect of *CTGF*-siRNA observed in KK and ES-2 cells may not be caused by off-target effects of siRNA used in this study.

Discussion

In this study, we identified a homozygous deletion of *CTGF* at 6q23.2 in ovarian cancer cell lines by array-CGH analysis using an in-house BAC array. Expression of *CTGF* was detected in normal ovary and a normal ovarian epithelial cell–derived cell line but frequently silenced through methylation of CpG sites around the *CTGF* CpG island exhibiting promoter activity in our panel of ovarian cancer cell lines, suggesting that *CTGF* may be one of targets for inactivation in ovarian cancer, although possible involvement of other target gene(s) for the homozygous loss at 6q23.1 remains unclear. Hypermethylation of the *CTGF* promoter region was frequently detected in primary ovarian cancers. Lower CTGF protein levels were frequently observed in primary ovarian cancers, although the clinical significance of CTGF expression might differ among disease stages and histologic subtypes. In addition, the transient transfection of *CTGF* or treatment with recombinant CTGF had an inhibitory effect on growth of *CTGF*-nonexpressing ovarian cancer cells, whereas knockdown of CTGF using siRNA accelerated growth of

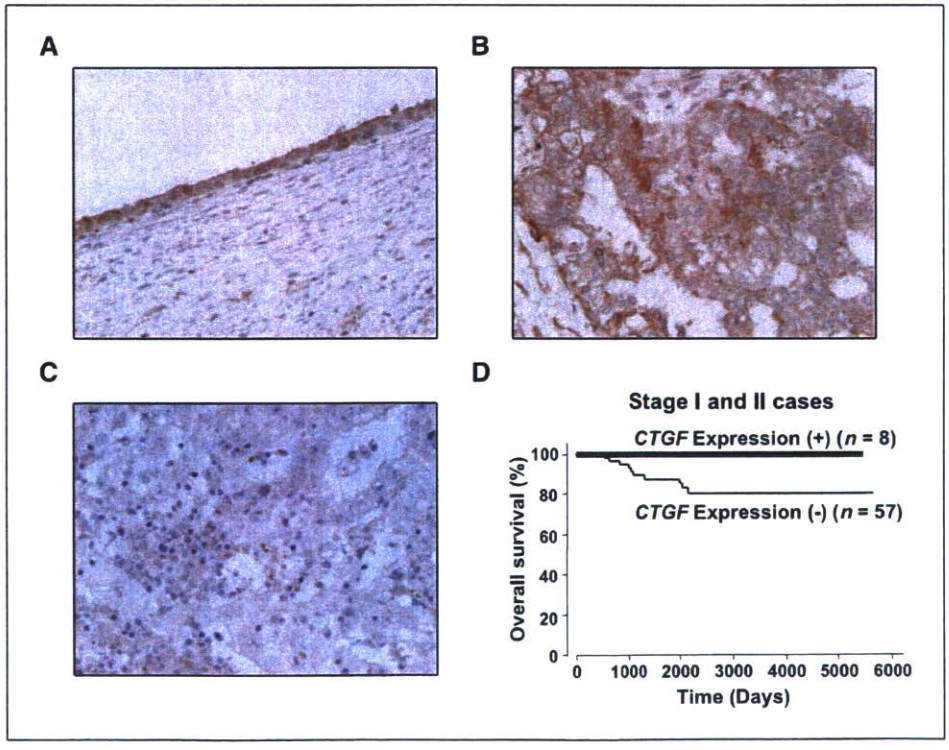

Figure 3. Immunohistochemical analysis of CTGF expression in primary ovarian cancer tumors. *A*, representative CTGF immunohistochemical staining of normal human ovarian epithelial cells. High CTGF expression is shown in normal ovarian epithelial cells. Magnification, ×200. *B* and *C*, representative CTGF immunohistochemical staining of primary ovarian cancer cells. High (*B*) or almost no (*C*) expression of CTGF was observed in primary ovarian cancer cells. In normal epithelial cells and ovarian cancer cells, CTGF is localized distinctly in the apical cytoplasm. Magnification, ×200. *D*, Kaplan-Meier curve for overall survival rates of patients with stage I and II ovarian cancer. There were no deaths in patients with stage I and II ovarian cancers showing higher CTGF levels.

Table 2. Correlation between clinical background and expression of CTGF protein

	n	Expression of CTGF*	*P*†
		n (%)	
Total	103	19 (18)	
Age (y)			
<60	71	15 (21)	0.388
≥60	32	4 (13)	
FIGO stage			
I and II	66	8 (12)	**0.027**
III and IV	37	11 (30)	
Histologic type			
Serous	42	8 (19)	**0.029**
Mucinous	15	7 (47)	
Clear cell	34	2 (6)	
Endometrioid	12	2 (17)	
Optimal surgery (cm)			
Optimal (<2)	82	16 (20)	1.000
Suboptimal (≥2)	14	2 (14)	
Unknown	7	1 (14)	
Peritoneal cytology			
Positive	48	11 (23)	0.387
Negative	50	8 (16)	
Unknown	5	0 (0)	
Methylation‡			
Positive	33	6 (18)	0.739
Negative	22	5 (23)	
Unknown	48	8 (17)	

NOTE: Statistically significant values are in boldface type.
* CTGF protein expression was evaluated by immunohistochemical analysis described in Materials and Methods.
† *P* values are from χ^2 or Fisher's exact test and were statistically significant when <0.05 (two sided).
‡ Methylation status was determined by MSP target for region 2A described in Materials and Methods.

CTGF-expressing ovarian cancer cells. These results suggest that loss of epigenetic inactivation of CTGF plays a pivotal role in the tumorigenesis of ovarian epithelial cells.

CTGF is a member of the CCN family, which comprises CTGF, cysteine-rich 61 (Cyr61/CCN1), nephroblastoma overexpressed (Nov/CCN3), Wisp-1/elm1 (CCN4), Wisp-2/rCop1 (CCN5), and Wisp-3 (CCN6). Among them, CTGF is believed to be a multifunctional signaling modulator involved in a wide variety of biological or pathologic processes, such as angiogenesis, osteogenesis, and renal and skin disorders (32–35). In carcinogenesis, CTGF was shown to be a positive regulator: the level of CTGF expression is positively correlated with bone metastasis in breast cancer (36), glioblastoma growth (37), a poor prognosis in esophageal adenocarcinomas (38), the aggressive behavior of pancreatic cancer cells (39), the invasive melanoma (40), and prognosis of chondrosarcoma (41). On the other hand, there is a body of evidence showing antigrowth (16, 42, 43) or antimetastatic (15) activity of CTGF in cancer cells and decreased CTGF expression in the aggressive or metastatic phenotype in various cancers, such as breast, colon, and NSCLCs (15, 16, 45). Given our results showing a tumor-suppressive function of CTGF, the role of CTGF in various cancers seems to vary considerably, depending on the tissues involved, although the exact mechanism has not yet been clarified. The question of how the tissue context is able to determine the action of CTGF in carcinogenesis deserves further investigation.

CTGF is located at 6q23.1, a chromosomal region that is rarely involved in copy number losses (22, 27–29). Indeed, most of the ovarian cancer cell lines used in this study showed normal DNA copy numbers around this region. Among 12 cell lines that showed reduced expression of *CTGF*, 9 lines had promoter hypermethylation, only 1 line showed both hemizygous deletion around this gene and promoter hypermethylation, whereas 2 lines showed neither, suggesting that the inactivation of CTGF might occur frequently through methylation of both alleles during the tumorigenesis of ovarian cancer. DNA methylation around the *CTGF* gene has also been reported in other cancers, such as hepatocellular carcinoma (17, 18) and colon cancer cell lines (19), suggesting that *CTGF* might be a universal target for methylation in various types of cancers. However, (*a*) some ovarian cancer cell lines showed reduced *CTGF* expression without DNA methylation and (*b*) silencing of CTGF protein expression occurs more frequently compared with DNA methylation of the *CTGF* gene in primary ovarian cancer, suggesting that mechanisms other than DNA methylation also contribute to silencing of CTGF in ovarian cancer. Recently, miR-17-92, especially miR-18, was shown to be responsible for CTGF down-regulation in Myc-transduced RAS-transformed mice colonocytes (30). Therefore, further analyses will be needed to clarify all mechanisms for silencing CTGF expression and determine the functional significance of each mechanism in primary ovarian cancer.

In our promoter assays, the *CTGF* CpG island around exons 1 and 2, especially fragment 3 from exon 1 to the middle of exon 2, whose methylation status was inversely related with expression status in ovarian cancer cells, showed clear promoter activity, whereas fragment 2 from the middle of exon 2 to exon 3, which was highly methylated in ovarian cancer cells regardless of expression status, showed weaker promoter activity. It was reported that the commonly methylated region within the *CTGF* CpG island starts from the middle of exon 1 and its methylation seems to be inversely correlated with *CTGF* expression in hepatocellular carcinoma cell lines (17, 18), and exonic methylation is observed in colon cancer cell lines with increased expression of *CTGF* caused by 5-aza-dCyd treatment (19), although methylation status of CpG sites through the entire CpG island and its correlation with gene expression was not clearly shown (17–19). Those results suggest that methylation of CpG sites within fragment 3/region 2A might be responsible for the silencing of *CTGF*, although few studies have shown that promoter activity can occur in fragments, especially CpG islands, not containing a 5′ sequence around transcription start sites (9, 46–48).

In the present study, little or no immunoreactivity for CTGF protein was observed in most primary ovarian cancers, especially in the earlier stages, which is contrary to the previously reported finding that low-level immunoreactivity was usually observed in advanced stage of colorectal cancers (15). In the earlier stages of ovarian cancer, moreover, patients with tumors showing lower CTGF immunoreactivity tended to have a worse survival rate than those showing higher levels of expression. Because we showed that (*a*) normal ovarian epithelia and immortalized ovarian epithelial cell–derived cell line express CTGF and (*b*) induction of *CTGF* expression or treatment of recombinant CTGF inhibited growth of *CTGF*-nonexpressing ovarian cancer cells, it is suggested that frequent silencing of *CTGF* occurred as an early event in ovarian

cancers at least partly through promoter methylation may contribute to the progression to an advanced stage. In the advanced stages, on the other hand, *CTGF* expression might be restored and contribute to more malignant phenotypes, such as invasion and metastasis, although the number of cases was too small to provide any conclusive results in the statistical analysis. In a breast cancer model (36), *CTGF* was identified as one of the genes contributing to bone metastagenicity, and its expression was transcriptionally induced by transforming growth factor β (TGFβ), which can have direct pro-oncogenic effects on tumor cells by stimulating their invasion and metastasis at least partially by inducing epithelial-to-mesenchymal transition in the later stages of carcinogenesis, when cancer cells have become insensitive to TGFβ-induced growth inhibition and apoptosis (36, 49). Therefore, it is possible that CTGF expression might be induced or restored by TGFβ to acquire an invasive/metastatic phenotype in advanced ovarian cancers without *CTGF* methylation. Because the silencing of *CTGF* occurs in a subset of ovarian cancer and may affect various biological functions in a stage-dependent and/or histologic subtype-dependent manner, evaluation of the methylation and/or expression status of *CTGF* with disease stage and/or histologic subtype might be useful for predicting the progression or

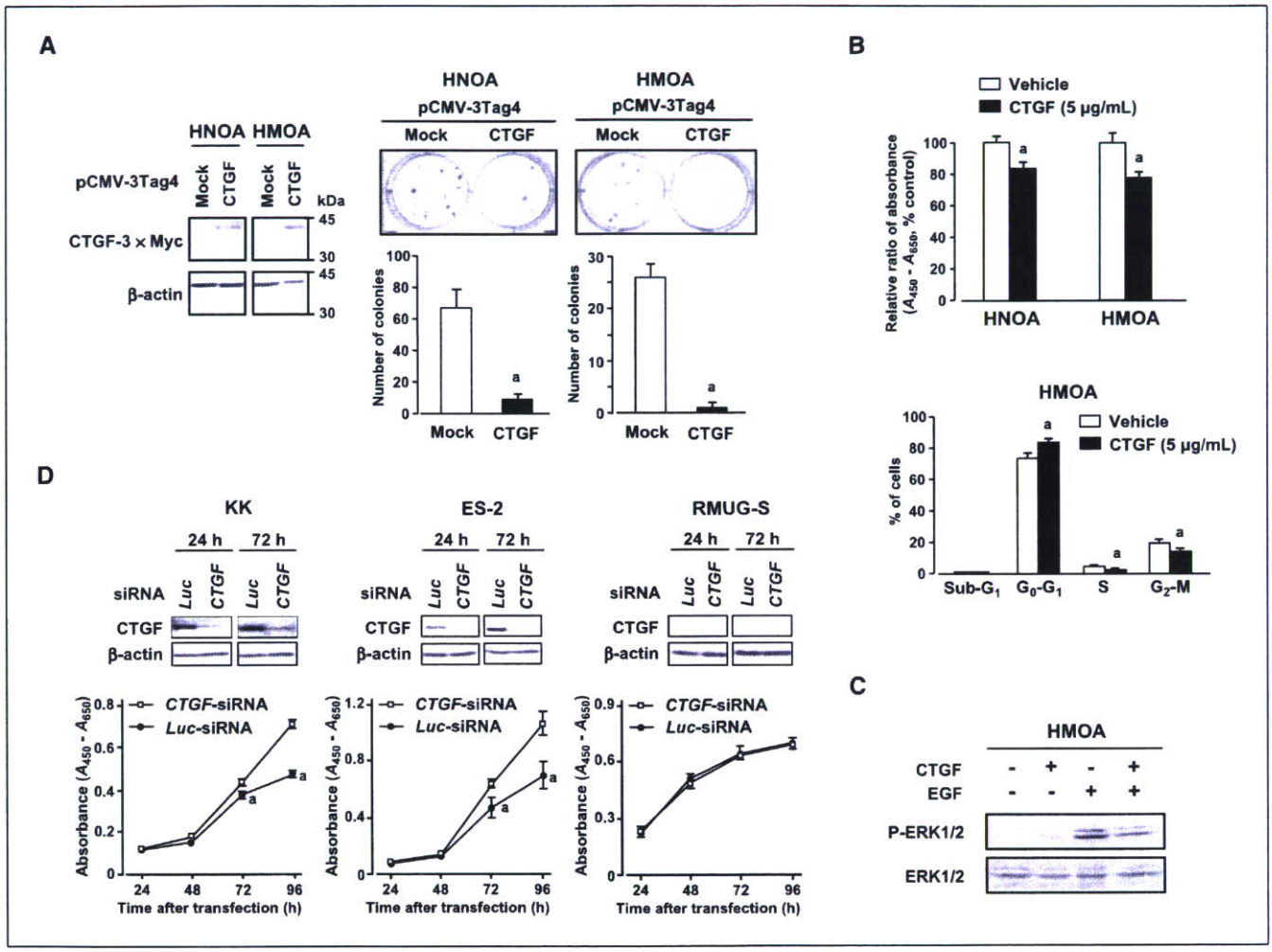

Figure 4. *A*, effects of restoration of CTGF expression on growth of ovarian cancer cells. Colony formation assays were done using ovarian cancer cell lines lacking expression of *CTGF*. Cells were transiently transfected with a Myc-tagged construct containing *CTGF* (pCMV-3Tag4-CTGF), or empty vector (mock), and selected for 2 wks with appropriate concentrations of G418. *Left*, Western blot prepared with 10 μg of protein extract and anti-Myc antibody, showing that cells transiently transfected with pCMV-3Tag4-CTGF expressed Myc-tagged CTGF. *Right, top*, 2 wks after transfection and subsequent selection of drug-resistant colonies, the colonies formed by *CTGF*-transfected cells were less numerous than those formed by mock-transfected cells. *Right, bottom*, quantitative analysis of colony formation. Colonies >2 mm were counted. *Columns*, mean of three separate experiments, each done in triplicate (histogram); *bars*, SD. *a*, $P < 0.05$, statistical analysis used the Mann-Whitney *U* test. *B*, effects of recombinant human CTGF on growth of ovarian cancer cells. Ovarian cancer cells lacking expression of *CTGF* (HNOA and HMOA) were treated with 2.5 μg/mL of recombinant human CTGF or vehicle (PBS) alone for 72 h. *Top*, cell viability was determined by WST assay in both cell lines; *bottom*, the population in each phase of cell cycle was assessed by FACS using HMOA cell line. Similar result was obtained in HNOA cell line (data not shown). *Columns*, mean of triplicate experiments; *bars*, SD. *a*, $P < 0.05$, statistical analysis used the Mann-Whitney *U* test. *C*, representative result of Western blotting for P-ERK1/2 and total ERK (ERK1/2) in HMOA cell line. HMOA cells were serum starved for 24 h, pretreated with CTGF (2.5 μg/mL) or vehicle (PBS) for 1 h, and then stimulated with EGF (25 ng/mL) of vehicle (PBS) for additional 15 min. ERK activation was evaluated by the amount of P-ERK determined by Western blotting. Similar result was obtained in HNOA cell line (data not shown). *D*, effect of knockdown of endogenous CTGF on growth of ovarian cancer cells. Fifty nanomol per liter of *CTGF*-specific siRNA (*CTGF*-siRNA) or a control siRNA for the *luciferase* gene (*Luc*-siRNA) were transfected into ovarian cancer cell lines expressing (KK and ES-2) or lacking (RMUG-S) CTGF, and the numbers of viable cells after transfection were assessed at the indicated times by WST assay. *Points*, mean of triplicate experiments; *bars*, SD. *a*, $P < 0.05$, statistical analysis used the Mann-Whitney *U* test.

aggressiveness of this disease. Further examination using a larger set of ovarian cancer cases will be needed to test our supposition that CTGF has two conflicting functions during tumorigenesis and inactivation of CTGF at least partly due to DNA methylation is a frequent and important event in the early progression of ovarian cancer.

In functional analyses, we showed that ectopically expressed CTGF or treatment with recombinant CTGF inhibits growth of *CTGF*-nonexpressing ovarian cancer cells, whereas knockdown of CTGF promotes growth of *CTGF*-expressing ovarian cancer cells. Similar results were obtained in cell lines of other types of cancer, such as NSCLC (16) and breast cancer (43). Chien et al. (16) showed that the growth of NSCLC cell lines expressing wild-type p53 was suppressed by forced expression of CTGF, likewise Cyr61, another member of the CCN family (50), although they have provided no evidence that their growth-inhibitory activity is mediated through p53. In our study, CTGF-induced growth suppression was observed in ovarian cancer cell lines regardless of the mutation status of *TP53*, and mutation of *TP53* was similarly observed in both *CTGF*-expressing and *CTGF*-nonexpressing ovarian cancer cell lines, suggesting that the growth-inhibitory activity of CTGF may not be affected by the mutation status of *TP53* in ovarian cancer. Because CTGF may exert growth-inhibiting activity at least partly through inhibition of the EGF-induced phosphorylation of ERK1/2 in NSCLC (16) and ovarian cancer (Fig. 4*C*), whereas it was shown that *CTGF* expression was inversely correlated with invasiveness/metastasis but not with cell growth in colorectal cancer (15), it is possible that CTGF affects different cellular functions in a cell- or tissue lineage–dependent manner.

Acknowledgments

Received 12/12/2006; revised 5/16/2007; accepted 5/24/2007.

Grant support: Grants-in-Aid for Scientific Research on Priority Areas and the 21st Century Center of Excellence Program for Molecular Destruction and Reconstitution of Tooth and Bone from the Ministry of Education, Culture, Sports, Science, and Technology, Japan and a grant-in-aid from Core Research for Evolutional Science and Technology of the Japan Science and Technology Corp.

The costs of publication of this article were defrayed in part by the payment of page charges. This article must therefore be hereby marked *advertisement* in accordance with 18 U.S.C. Section 1734 solely to indicate this fact.

We thank Dr. Hidetaka Katabuchi for providing the OSE-2a cell line and Ayako Takahashi and Rumi Mori for technical assistance.

References

1. Jemal A, Siegel R, Ward E, et al. Cancer Statistics, 2006. CA Cancer J Clin 2006;56:106–30.
2. Ozols RF, Bookman MA, Connolly DC, et al. Focus on epithelial ovarian cancer. Cancer Cell 2004;5:19–24.
3. Prowse A, Frolov A, Godwin AK. The genetics of ovarian cancer. In: Ozols RF, editor. American Cancer Society Atlas of Clinical Oncology. Hamilton (Ontario): B.C. Decker. Inc.; 2003. p. 49–82.
4. Friend SH, Bernards R, Rogelj S, et al. A human DNA segment with properties of the gene that predisposes to retinoblastoma and osteosarcoma. Nature 1986;323:643–6.
5. Kamb A, Gruis NA, Weaver-Feldhaus J, et al. A cell cycle regulator potentially involved in genesis of many tumor types. Science 1994;264:436–40.
6. Hahn SA, Schutte M, Hoque AT, et al. DPC4, a candidate tumor suppressor gene at human chromosome 18q21.1. Science 1996;271:350–3.
7. Jones PA, Baylin SB. The fundamental role of epigenetic events in cancer. Nat Rev Genet 2002;3:415–28.
8. Inazawa J, Inoue J, Imoto I. Comparative genomic hybridization (CGH)-arrays pave the way for identification of novel cancer-related genes. Cancer Sci 2004;95:559–63.
9. Sonoda I, Imoto I, Inoue J, et al. Frequent silencing of low density lipoprotein receptor-related protein 1B (LRP1B) expression by genetic and epigenetic mechanisms in esophageal squamous cell carcinoma. Cancer Res 2004;64:3741–7.
10. Imoto I, Izumi H, Yokoi S, et al. Frequent silencing of the candidate tumor suppressor PCDH20 by epigenetic mechanism in non-small-cell lung cancers. Cancer Res 2006;66:4617–26.
11. Katsaros D, Cho W, Singal R, et al. Methylation of tumor suppressor gene p16 and prognosis of epithelial ovarian cancer. Gynecol Oncol 2004;94:685–92.
12. Agathanggelou A, Honorio S, Macartney DP, et al. Methylation associated inactivation of RASSF1A from region 3p21.3 in lung, breast, and ovarian tumours. Oncogene 2001;20:1509–18.
13. Catteau A, Harris WH, Xu CF, Solomon E. Methylation of the BRCA1 promoter region in sporadic breast and ovarian cancer: correlation with disease characteristics. Oncogene 1999;18:1957–65.
14. Geisler JP, Goodheart MJ, Sood AK, Holmes RJ, Hatterman-Zogg MA, Buller RE. Mismatch repair gene expression defects contribute to microsatellite instability in ovarian carcinoma. Cancer 2003;98:2199–206.
15. Lin BR, Chang CC, Che TF, et al. Connective tissue growth factor inhibits metastasis and acts as an independent prognostic marker in colorectal cancer. Gastroenterology 2005;128:9–23.
16. Chien W, Yin D, Gui D, et al. Suppression of cell proliferation and signaling transduction by connective tissue growth factor in non-small cell lung cancer cells. Mol Cancer Res 2006;4:591–8.
17. Chiba T, Yokosuka O, Arai M, et al. Identification of genes up-regulated by histone deacetylase inhibition with cDNA microarray and exploration of epigenetic alterations on hepatoma cells. J Hepatol 2004;41:436–45.
18. Chiba T, Yokosuka O, Fukai K, et al. Identification and investigation of methylated genes in hepatoma. Eur J Cancer 2005;41:1185–94.
19. Hayashi H, Nagae G, Tsutsumi S, et al. High-resolution mapping of DNA methylation in human genome using oligonucleotide tiling array. Hum Genet 2007;120:701–11.
20. Kikuchi Y, Miyauchi M, Kizawa I, Oomori K, Kato K. Establishment of a cisplatin-resistant human ovarian cancer cell line. J Natl Cancer Inst 1986;77:1181–5.
21. Hirata J, Kikuchi Y, Kita T, et al. Modulation of sensitivity of human ovarian cancer cells to *cis*-diamminedichloroplatinum(II) by 12-*O*-tetradecanoylphorbol-13-acetate and DL-buthionine-S,R-sulphoximine. Int J Cancer 1993;55:521–7.
22. Watanabe T, Imoto I, Kosugi Y, et al. A novel amplification at 17q21-23 in ovarian cancer cell lines detected by comparative genomic hybridization. Gynecol Oncol 2001;81:172–7.
23. Nitta M, Katabuchi H, Ohtake H, Tashiro H, Yamaizumi M, Okamura H. Characterization and tumorigenicity of human ovarian surface epithelial cells immortalized by SV40 large T antigen. Gynecol Oncol 2001;81:10–7.
24. Saigusa K, Imoto I, Tanikawa C, et al. RGC32, a novel p53-inducible gene, is located on centrosomes during mitosis and results in G_2/M arrest. Oncogene 2007;26:1110–21.
25. Xiong Z, Laird PW. COBRA: a sensitive and quantitative DNA methylation assay. Nucleic Acids Res 1997;25:2532–4.
26. Imoto I, Tsuda H, Hirasawa A, et al. Expression of cIAP1, a target for 11q22 amplification, correlates with resistance of cervical cancers to radiotherapy. Cancer Res 2002;62:4860–6.
27. Iwabuchi H, Sakamoto M, Sakunaga H, et al. Genetic analysis of benign, low-grade, and high-grade ovarian tumors. Cancer Res 1995;55:6172–80.
28. Arnold N, Hagele L, Walz L, et al. Overrepresentation of 3q and 8q material and loss of 18q material are recurrent findings in advanced human ovarian cancer. Genes Chromosomes Cancer 1996;16:46–54.
29. Sonoda G, Palazzo J, du Manoir S, et al. Comparative genomic hybridization detects frequent overrepresentation of chromosomal material from 3q26, 8q24, and 20q13 in human ovarian carcinomas. Genes Chromosomes Cancer 1997;20:320–8.
30. Dews M, Homayouni A, Yu D, et al. Augmentation of tumor angiogenesis by a Myc-activated microRNA cluster. Nat Genet 2006;38:1060–5.
31. Berchuck A, Rodriguez GC, Kamel A, et al. Epidermal growth factor receptor expression in normal ovarian epithelium and ovarian cancer. I. Correlation of receptor expression with prognostic factors in patients with ovarian cancer. Am J Obstet Gynecol 1991;164:669–74.
32. Brigstock DR. The connective tissue growth factor/cysteine-rich 61/nephroblastoma overexpressed (CCN) family. Endocr Rev 1999;20:189–206.
33. Lau LF, Lam SC. The CCN family of angiogenic regulators the integrin connection. Exp Cell Res 1999;248:44–57.
34. Perbal B. The CCN family of genes a brief history. Mol Pathol 2001;54:103–4.
35. Perbal B. NOV (nephroblastoma overexpressed) and the CCN family of genes structural and functional issues. Mol Pathol 2001;54:57–79.
36. Kang Y, Siegel PM, Shu W, et al. A multigenic program mediating breast cancer metastasis to bone. Cancer Cell 2003;3:537–49.
37. Pan LH, Beppu T, Kurose A, et al. Neoplastic cells and proliferating endothelial cells express connective tissue growth factor (CTGF) in glioblastoma. Neurol Res 2002;24:677–83.
38. Koliopanos A, Friess H, di Mola FF, et al. Connective tissue growth factor gene expression alters tumor progression in esophageal cancer. World J Surg 2002;26:420–7.
39. Wenger C, Ellenrieder V, Alber B, et al. Expression and differential regulation of connective tissue growth factor in pancreatic cancer cells. Oncogene 1999;18:1073–80.
40. Kubo M, Kikuchi K, Nashiro K, et al. Expression of fibrogenic cytokines in desmoplastic malignant melanoma. Br J Dermatol 1998;139:192–7.
41. Shakunaga T, Ozaki T, Ohara N, et al. Expression of connective tissue growth factor in cartilaginous tumors. Cancer 2000;89:1466–73.
42. Moritani NH, Kubota S, Nishida T, et al. Suppressive effect of overexpressed connective tissue growth

factor on tumor cell growth in a human oral squamous cell carcinoma-derived cell line. Cancer Lett 2003;192: 205–14.
43. Hishikawa K, Oemar BS, Tanner FC, Nakaki T, Luscher TF, Fujii T. Connective tissue growth factor induces apoptosis in human breast cancer cell line MCF-7. J Biol Chem 1999;274:37461–6.
44. Jiang WG, Watkins G, Fodstad O, Douglas-Jones A, Mokbel K, Mansel RE. Differential expression of the CCN family members Cyr61, CTGF, and Nov in human breast cancer. Endocr Relat Cancer 2004;11:781–91.
45. Planque N, Perbal B. A structural approach to the role of CCN (CYR61/CTGF/NOV) proteins in tumourigenesis. Cancer Cell Int 2003;3:1–15.
46. Misawa A, Inoue J, Sugino Y, et al. Methylation-associated silencing of the nuclear receptor 112 gene in advanced-type neuroblastomas, identified by bacterial artificial chromosome array-based methylated CpG island amplicon. Cancer Res 2005;65:10233–42.
47. Kolb A. The first intron of the murine β-casein gene contains a functional promoter. Biochem Biophys Res Commun 2003;306:1099–105.
48. Nakagawachi T, Soejima H, Urano T, et al. Silencing effect of CpG island hypermethylation and histone modifications on *O6*-methylguanine-DNA methyltransferase (MGMT) gene expression in human cancer. Oncogene 2003;22:8835–44.
49. Deckers M, van Dinther M, Buijs J, et al. The tumor suppressor Smad4 is required for transforming growth factor β-induced epithelial to mesenchymal transition and bone metastasis of breast cancer cells. Cancer Res 2006;66:2202–9.
50. Tong X, Xie D, O'Kelly J, Miller CW, Muller-Tidow C, Koeffler HP. Cyr61, a member of CCN family, is a tumor suppressor in non-small cell lung cancer. J Biol Chem 2001;276:47709–14.

Genome-wide array-based comparative genomic hybridization analysis of pancreatic adenocarcinoma: Identification of genetic indicators that predict patient outcome

Panayiotis Loukopoulos,[1,7] Tatsuhiro Shibata,[1,2,8] Hiroto Katoh,[1,2] Akiko Kokubu,[1,2] Michiie Sakamoto,[3] Ken Yamazaki,[3] Tomoo Kosuge,[4] Yae Kanai,[1] Fumie Hosoda,[2] Issei Imoto,[5,6] Misao Ohki,[2] Jyoji Inazawa[5,6] and Setsuo Hirohashi[1]

[1]Pathology Division, and [2]Cancer Genomics Project, National Cancer Center Research Institute, 51-1, Tsukiji, Chuo-ku, Tokyo 1040-045; [3]Department of Pathology, Keio University School of Medicine, 35 Shinanomachi, Shinjuku-ku, Tokyo 1600-016; [4]Department of Hepato-Biliary-Pancreatic Surgery, National Cancer Center, Hospital, 51-1, Tsukiji, Chuo-ku, Tokyo 1040-045; [5]Department of Molecular Cytogenetics, Medical Research Institute, Tokyo Medical and Dental University, 15-45 Yushima, Bunkyo-ku, Tokyo 1138-519; [6]Core Research for Evolutionary Science and Technology (CREST) of the Japan Science and Technology (JST) Corporation, 41-8 Hon-machi Kawaguchi, Saitama 3320-012, Japan

(Received August 1, 2006/Revised November 17, 2006/Accepted November 19, 2006/Online publication January 8, 2007)

We analyzed the subchromosomal numerical aberrations of 44 surgically resected pancreatic adenocarcinomas by array-based comparative genomic hybridization. The aberration profile ranged widely between cases, suggesting the presence of multiple or complementary mechanisms of evolution in pancreatic cancer, and was associated with lymph node metastasis and venous or serosal invasion. A large number of small loci, previously uncharacterized in pancreatic cancer, showed non-random loss or gain. Frequent losses at 1p36, 4p16, 7q36, 9q34, 11p15, 11q13, 14q32-33, 16p13, 17p11-13, 17q11-25, 18q21-tel, 19p13, 21q22 and 22q11-12, and gains at 1q25, 2p16, 2q21-37, 3q25, 5p14, 5q11-13, 7q21, 7p22, 8p22, 8q21-23, 10q21, 12p13, 13q22, 15q13-22 and 18q11 were identified. Sixteen loci were amplified recurrently. We identified novel chromosomal alterations that were significantly associated with a range of malignant phenotypes. Gain of LUNX, HCK, E2F1 and DNMT3b at 20q11, loss of p73 at 1p36 and gain of PPM1D at 17q23 independently predicted patient outcome. Expression profiling of amplified genes identified Smurf1 and TRRAP at 7q22.1, BCAS1 at 20q13.2-3, and VCL at 10q22.1 as potential novel oncogenes. Our results contribute to a complete description of genomic structural aberrations and the identification of potential therapeutic targets and genetic indicators that predict patient outcome in pancreatic adenocarcinoma. (*Cancer Sci* 2007; 98: 392–400)

Pancreatic adenocarcinoma is a leading cause of cancer-related death worldwide; the 5-year survival rate for patients that underwent surgery remains below 5%.[1] Pancreatic adenocarcinoma appears to successively acquire genetic aberrations in genes involved in the regulation of cell proliferation, the central ones being early activating mutations of the K-ras oncogene, followed by inactivation of the p53, p16 and DPC4 TSG.[2] The application of chromosome CGH,[3] karyotype and allelotype studies in pancreatic cancer has also revealed a large number of complex structural and numerical aberrations at the subchromosomal level.[4–11] Recurrent aberrations reported concern copy number gain on 3q, 5p, 7p, 8q, 11q, 12p, 17q, 19q and 20q and loss on 1p, 3p, 4q, 6q, 8p, 9p, 10q, 12q, 13q, 15q, 17p, 18q, 19p, 21q and 22q.[8,12] aCGH methods have recently been developed and used in studies of various malignancies, including pancreatic cancer. The latter used cell lines,[13–18] and a small number of primary cases[14,15] or xenografts,[19] to confirm previously described regional alterations and identify novel ones. Although some of these loci are known to contain oncogenes or TSG,[2] the role that copy number alterations of most of the above loci play in pancreatic cancer genesis or progression, if any, is far from being fully evaluated. From these and previous studies, it is also evident that there exists substantial variation in the reported aberrations between studies as well as between individual cases.

The aim of the present study was to examine the SNAP of pancreatic cancer to identify novel loci that contain genes for which copy number status is likely to be relevant to pancreatic carcinogenesis or associated with clinically relevant parameters. For this, we used aCGH to examine a comparatively large number of well-characterized primary cases and LCM to allow more accurate analysis. In addition, mRNA expression analysis of loci exhibiting amplifications was carried out to identify genes that are amplified recurrently and overexpressed in pancreatic cancer.

Materials and Methods

Tumor samples. Forty-four methanol-fixed pancreatic ductal adenocarcinomas from 43 patients were examined (Suppl. Table 1). These included 33 specimens from patients who had undergone surgery at the National Cancer Center Hospital between 1994 and 2003, and 11 xenografts that were produced following the orthotopic implantation of tumors in severe combined immunodeficient mice, as described previously.[20] Forty-two samples were of primary tumors, one of a liver metastasis and one of a pancreatic xenograft of a liver metastasis, the corresponding primary of which was also examined. Tumor classification was carried out according to the Japan Pancreas Society guidelines.[21] The study was approved by the institutional review board of the National Cancer Center.

LCM and whole-genome amplification. LCM was carried out with a PixCell II (Arcturus Engineering, Mountain View, CA, USA). At least 5000 tumor cells per sample were recovered. Genomic (test) DNA was extracted by standard procedures. Sex-matched high molecular weight human genomic DNA (Promega, Madison, WI, USA) was sheared randomly (HydroShear; Gene Machines, San Carlos, CA, USA) and used as reference DNA. Both test and reference DNA were amplified

[8]To whom correspondence should be addressed. E-mail: tashibat@ncc.go.jp
[7]Present address: Pathology Division, Faculty of Veterinary Medicine, Aristotle University, Thessaloniki 54124, Greece.
Abbreviations: aCGH, array-based comparative genomic hybridization; BAC, bacterial artificial chromosome; CGH, comparative genomic hybridization; HD, homozygous deletion; LCM, laser-capture microdissection; PCR, polymerase chain reaction; SNAP, subchromosomal numerical aberration profile; TSG, tumor suppressor gene.

doi: 10.1111/j.1349-7006.2007.00395.x

Fig. 1. Chromosomal copy number changes revealed by array-based comparative genomic hybridization. Representative array-based comparative genomic hybridization profile of a pancreatic adenocarcinoma. Copy number losses (ratio < 0.75) and gains (ratio > 1.25) were detected in both large fractions of the chromosome arms and small chromosomal regions. Amplifications (ratio > 2.00, arrowheads) and homozygous deletions (ratio < 0.25, arrow) were also identified in this tumor. The average signal ratios (test:reference) of two normalized signals from duplicated spots are given from chromosome 1p telomere (left) to Xq telomere (right). The vertical dotted and continuous lines indicate the position of the centromere and telomere of each chromosome, respectively.

using an adaptor ligation-mediated whole-genome PCR, as described previously.[22]

Array-based CGH. A custom-made CGH array ('MCG Cancer Array-800 ver. 2') was used, consisting of 800 duplicated target BAC clones that correspond to chromosomal loci of potential importance in various cancers (listed at http://www.cghtmd.jp/CGHDatabase/microarray/mcg800_array_e.htm). Labeling of the DNA probes, hybridization, data acquisition and data normalization were carried out as described previously.[23–25] Based on control experiments,[26] we considered a signal ratio <0.75 or >1.25 to indicate loss or gain, respectively, and a ratio of <0.25 or >2.00 to indicate HD or amplification, respectively.

The validity of our aCGH data was confirmed by fluorescence *in situ* hybridization, PCR (Suppl. Fig. 1), loss of heterozygosity analysis and immunohistochemistry for selected genes.[26]

Expression profiling of primary xenografts. We used xenografts for gene expression analysis due to their abundance in tumors cells compared with primary tumors. We focused on the relationship between amplification and overexpression; additional gene expression profiling results will be submitted in a subsequent publication.

Total RNA was extracted from frozen xenograft samples, biotin-labeled cRNA synthesized and hybridized to a probe array (HG-U95Av2, Affymetrix) and data acquired as described.[27] A probe set signal log ratio (SLR) of the gene expression level in the tumor relative to the control (normal pancreas) >1.5 was defined as indicating overexpression.

Statistical analysis. The χ^2 test was used to assess the statistical significance, set at 0.05, of intergroup differences in the frequency of aberrations of individual loci. The relationship between clinicopathological parameters and the number of aberrations per case was evaluated using Student's unpaired *t*-test. Survival curves were calculated using the Kaplan–Meier method, and differences in survival periods were analyzed with the log-rank test.

Results

Range of numerical aberrations. We constructed and analyzed the genomic profile of 44 pancreatic adenocarcinomas using aCGH. Subchromosomal numerical aberrations were revealed in all but two (42/44) of the tumors examined (Fig. 1). The number of aberrations differed widely between cases (Suppl. Table 2; Suppl. Fig. 2). Apart from the two cases in which no copy number changes were observed, a third case showed changes in only 11 loci (all gains), whereas nine cases (20%) had alterations in more than 50% of loci. In most cases (34/44), the number of gains was higher than the number of losses ($P < 10^{-7}$). Overall, however, the loss rate was similar to the gain rate (19% of loci altered on average per case for both). Similarly, amplifications were observed more frequently, in terms of number of cases and number of aberrations per case, than HD. Most loci showed aberrations in at least one case, the majority showing loss or gain in 2–25% and 0–20% of cases, respectively.

Loss. The most frequently lost loci were 17p13.3 (ABR, in 75% of cases), 18qtel (CTDP1, SHGC-145820, 68%) and 18q21 (SMAD7, 66%). The loci containing the p16 (9p21), p53 (17p13.1), SMAD4 and DCC (both at 18q21) genes were lost in 41, 55, 61 and 30% of cases, respectively. In total, 33 loci with frequent (>50%) losses were identified at 1p36, 4p16.3, 7q36, 9q34.3, 11p15, 11q13, 14q32-33, 16p13.3, 17p11.2, 17p13.1-3, 17q11-qter, 17q21.2, 17q25, 18q21, 18qtel, 19p13.2-3, 21q22.3, 22q11.23 and 22q12.1-2 (Fig. 2). The chromosome arms with the highest number of loci lost, taking into account only loci that were lost in >25% of cases, included, in descending order of frequency, 1p, 11q, 17p, 10q, 8p, 18q, 22q, 6q, 9p, 14q and 17q (Suppl. Table 3).

Homozygous deletions. Twenty-six loci with HD were detected, nine of which were in more than one case (Table 1). HD were detected in 11 cases (25%), seven of which in only one locus. The 1p35-36.33 region contained the highest number of loci deleted (six). The most frequently deleted locus was 9p21 spanning the p16 gene, whereas the locus containing SMAD4 (18q21) was deleted in one case.

Gains. Loci with frequent (>50% cases) gains were identified at 1q25.2-q25.3, 2p16, 2q21.2, 2q23-q37, 2q31, 2q33, 2q34, 3q25.1, 5p14.2, 5q11.2-q13.2, 7q21.1, 7p22, 8p22, 8q21, 8q22-q23, 10q21.1, 12p13.33, 13q22, 15q13-q22 and 18q11.2 (Fig. 2; Suppl. Table 4). The most frequently gained locus was 7q21.1 (71%) containing the HGF gene. The loci spanning the KRAS2 (12p12.1) and KRAG (12p11.2) genes were gained in 45 and 20% of cases, respectively. The NRAS (1p13), MYC (8q24), MDM2 (12q14.3) and AKT1 (14q32.2)[28] loci were gained in 45, 43, 36 and 18% of cases, respectively.

Amplifications. Amplifications were observed in 37 tumors. The seven cases in which no amplification was observed included six with few aberrations, and, interestingly, one case with 419 aberrations. Nineteen cases had amplifications in more than 1%, and three cases in more than 5% of loci examined.

Sixteen loci were amplified in five cases or more (>10%) (Table 2). The most frequently amplified locus was 18q11.2 containing RBBP8. 7q34 (BRAF) was amplified in four cases, whereas 12p12.1 (KRAS2), 1p13 (NRAS) and 8q24 (MYC) were amplified in two cases each.

Association of SNAP with clinicopathological parameters. A number of clinicopathological parameters were associated with the degree and type of aberration (Suppl. Table 5). Overall, cases with a phenotype indicating increased malignant potential had a higher degree of aberrations. Smaller tumors and tumors with higher venous or perineural invasion histological scores had a higher total number of aberrations than tumors that were larger or with lower invasion scores. No other clinicopathological parameters examined, such as the sex, primary tumor location, macroscopic type (infiltrative or nodular), degree of differentiation (Suppl. Table 6), infiltration or otherwise of certain neighboring tissues, pattern of such infiltration (INF α, β, or γ), or spread within the main pancreatic duct had significant correlation with SNAP (data not shown).

Association with venous invasion. Venous invasion-negative tumors had markedly different SNAP than venous invasion-positive tumors, although it should be noted that only a small number of negative tumors was examined. The loci lost or gained more frequently in the venous invasion-positive tumors are shown in

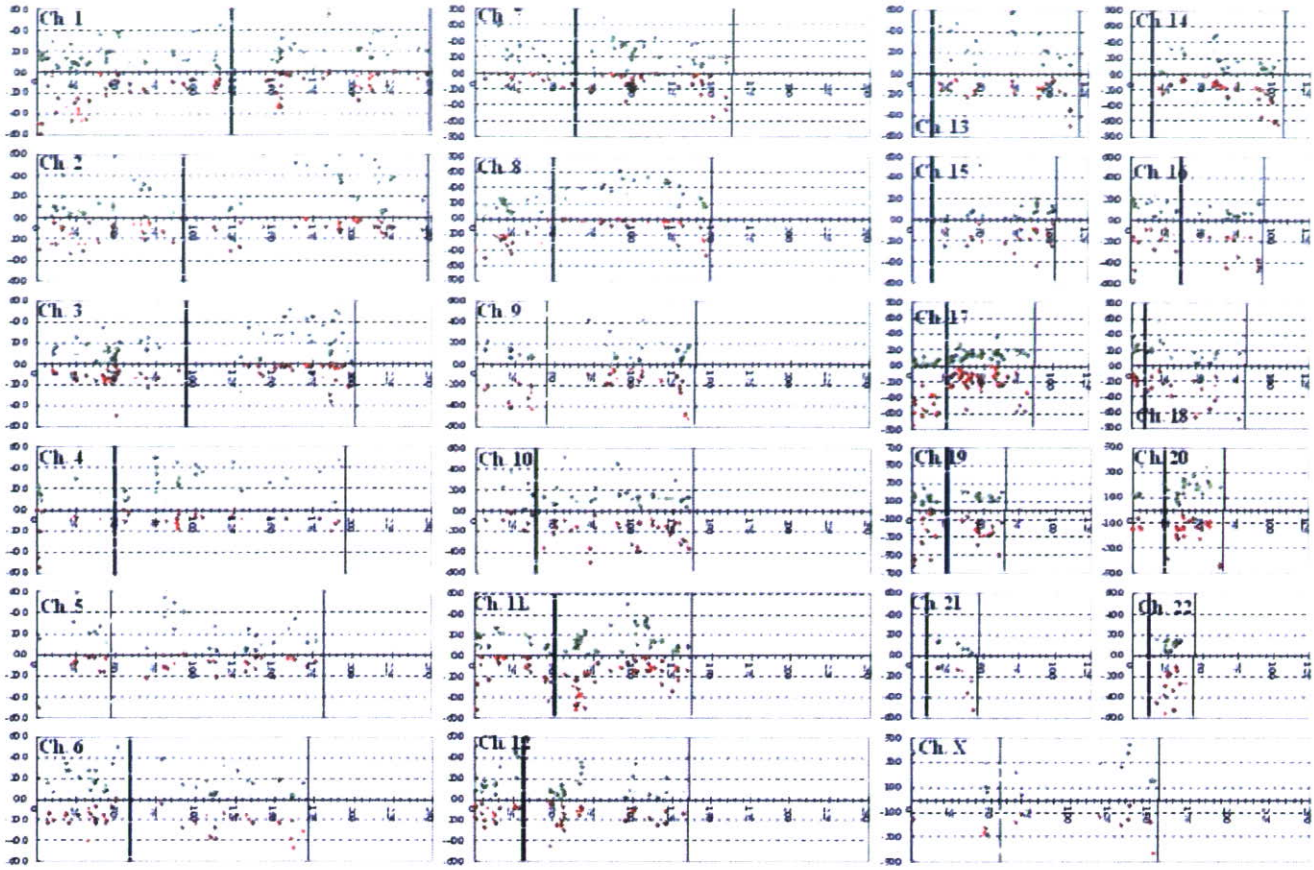

Fig. 2. Distribution of chromosomal copy number aberrations in pancreatic cancer. The horizontal axis indicates the physical distance (Mb) of the chromosomal loci from the telomere of the short arm. The vertical axis indicates the frequency (%) of tumors with chromosomal alterations (green, gain; red, loss). The vertical dotted and continuous lines indicate the positions of the centromere and telomere of each chromosome, respectively.

Table 1. Loci deleted homozygously in more than one case

Locus†	No. cases	Percentage of cases
9p21 (p16)	5	11
16p13.3 (ABCA3)	3	7
1p36.1 (p73)	2	5
5p15 (TERT)	2	5
11p15 (HRAS)	2	5
17q25 (MAFG)	2	5
18q21 (SMAD7)	2	5
18qtel (CTDP1,SHGC-145820)	2	5
19p13.3 (ABCA7)	2	5

†Known cancer-related genes contained in the respective clones are shown in parentheses.

Table 2. Loci amplified in more than 10% of cases

Locus†	No. cases	Percentage of cases
18q11.2 (RBBP8)	10	23
7q21.1 (HGF)	9	20
2q31 (PMS1)	7	16
11q13.3 (BCL1,FGF4)	7	16
2q34 (ERBB4)	6	14
11q13 (CCND1)	6	14
7q22.1 (Smurf1)	6	14
8q21 (NBS1)	5	11
2p16 (GTBP)	5	11
7p22 (ETV1)	5	11
2q21.2 (LRP1B)	5	11
2q35 (HUP2)	5	11
6q22 (ROS1)	5	11
8p11.2-p11.1 (FGFR1)	5	11
7q22.1 (CYP3A4)	5	11
7q22.1 (TRRAP)	5	11

†Known cancer-related genes contained in the respective clones are shown in parentheses.

Table 3. HD were not observed in the venous invasion-negative tumors (0/5 vs 19/37, $P = 0.03$). In the venous invasion-negative tumors, 178 and 84 loci, respectively, were lost or gained more frequently than in the positive tumors; these included frequently amplified loci (3/5) such as the ones containing FGF7 (15q13-q22), BRAF (7q34) ($P \leq 4.1 \times 10^{-5}$), ROS1 (6q22), GTBP (2p16) ($P = 0.0004$) and HGF (7q21.1) ($P = 0.02$).

Association with lymph node metastasis. Unlike venous invasion, few differences were observed when the genomic profiles of lymph node metastasis-positive and lymph node metastasis-negative tumors were compared, although only six negative tumors were examined. Only three loci showed significant differences in their signal ratios, 9p13 (SCYA21), 11q22 (ATM) and 17q12 (RAD51L3). Xq28 (MAGEA2) was lost more frequently in the lymph node metastasis-negative group (3/6 vs

doi: 10.1111/j.1349-7006.2007.00395.x

Table 3. Loci altered frequently in the venous invasion-positive pancreatic adenocarcinomas

Chromosomal locus	Contained cancer-related gene	Sub-chromosomal loss detected				*P* value†
		Venous invasion-positive cases		Venous invasion-negative cases		
		n	%	*n*	%	
19p13.3	ABCA7	26	70	0	0	0.002
9q34.3	ABCA2	25	68	1	20	0.040
1p36.33	TP73	22	59	0	0	0.012
11q13	FGF3	22	59	0	0	0.012
4p16	GAK	20	54	0	0	0.023
11q12	LTBP3	20	54	0	0	0.023
20q13	Livin	20	54	0	0	0.023
18q22	BCL2	19	51	0	0	0.030
5p14.2	CDH10	25	68	0	0	0.004
8q24	OPG	21	57	0	0	0.017
3q27-q29	TP63	20	54	0	0	0.023
8q24.1	NOV	20	54	0	0	0.023
14q22.3	RBBP1	19	51	0	0	0.030

†χ^2 test.

Table 4. Loci altered frequently in pancreatic adenocarcinoma cases with short-survival (<1 year) compared with long-survival periods

Chromosomal locus	Contained cancer-related gene	Sub-chromosomal loss detected				*P* value†
		Venous invasion-positive cases		Venous invasion-negative cases		
		n	%	*n*	%	
1p36.33	TP73	9	69	4	21	0.006
8q24.3	GLI4	5	38	1	5	0.018
Xq12	AR	5	38	1	5	0.018
11q13	STIP1, FOLR1	8	62	5	26	0.046
20q11.2	LUNX, TOP1	5	38	0	0	0.003
18p11.3	TGIF	6	46	1	5	0.006
4q13-q21	AREG	4	31	0	0	0.010
6q21	CCNC	4	31	0	0	0.010
10q21.1	PCDH15	10	77	6	32	0.012
1p32	RLF	5	38	1	5	0.018
2q36	Cul3	8	62	4	21	0.020
17q23	PPM1D	8	62	4	21	0.020
4q21	GRO1	6	46	2	11	0.022
1p36.2	KIAA0591(KIF1B)	7	54	3	16	0.023
4q21	GRO2	7	54	3	16	0.023
13q32	GPC5	7	54	3	16	0.023
8q22-q23	EIF3S6	9	69	6	32	0.036

†χ^2 test.

5/36, $P = 0.037$). Four loci, all on 7q21-22 (containing the HGF, DMTF1, MLL5 and CDK6 genes), were gained more frequently in the lymph node metastasis-positive group (all $P < 0.05$).

Association with survival. Thirty-two cases had survival data amenable to analysis. The genomic profiles of cases with a survival period shorter ($n = 13$) or longer than ($n = 19$) 1 year were compared. Four and 13 loci, respectively, were lost or gained more frequently in the short-compared with the long-survival group (Table 4). In contrast, only two loci were lost (6q25/ESR1 and 22q11.23/ADRBK2) and none gained more frequently in the long-compared with the short-survival group. Loss of 1p36 (p73) and 11q121-3 was associated with both short-term survival and evidence of venous invasion, whereas gain of 7q21-22 was associated with both short-term (<3 years) survival and the presence of lymph node metastases.

Kaplan–Meier analysis showed that loss of 1p36 (p73) ($P = 0.02$; Fig. 3a), gain of 17q23 (PPM1D) ($P < 0.05$; Fig. 3b) and particularly gain of the LUNX locus at 20q111-12 ($P < 0.0001$; Fig. 3c) were significantly associated with prognosis, whereas loss of the STIP1 or FOLR1 locus (11q13), gain of the TOP1 (20q11-12) and gain of MUC3 or Smurf1 loci (7q21-22) were not. Loci adjacent to LUNX on 20q11 were further analyzed; gain of the HCK ($P < 0.001$; Fig. 3d), E2F1 ($P < 0.005$; data not shown) and DNMT3b loci ($P < 0.05$; data not shown), but not TGIF2, were also associated with prognosis, albeit not as closely as LUNX.

Potential oncogenes revealed by expression profiling analysis. Eighty-one loci were amplified in at least one case in the group examined; these loci contained 15 genes that were overexpressed in at least one case (Table 5). Of the individual amplifications observed, 14.7% (20/136) resulted in overexpression. Only four genes were amplified and overexpressed in more than one case: Smurf1 (7q22.1), BCAS1 (20q13.2-3), which was the most frequently overexpressed, VCL (10q22.1) and TRRAP

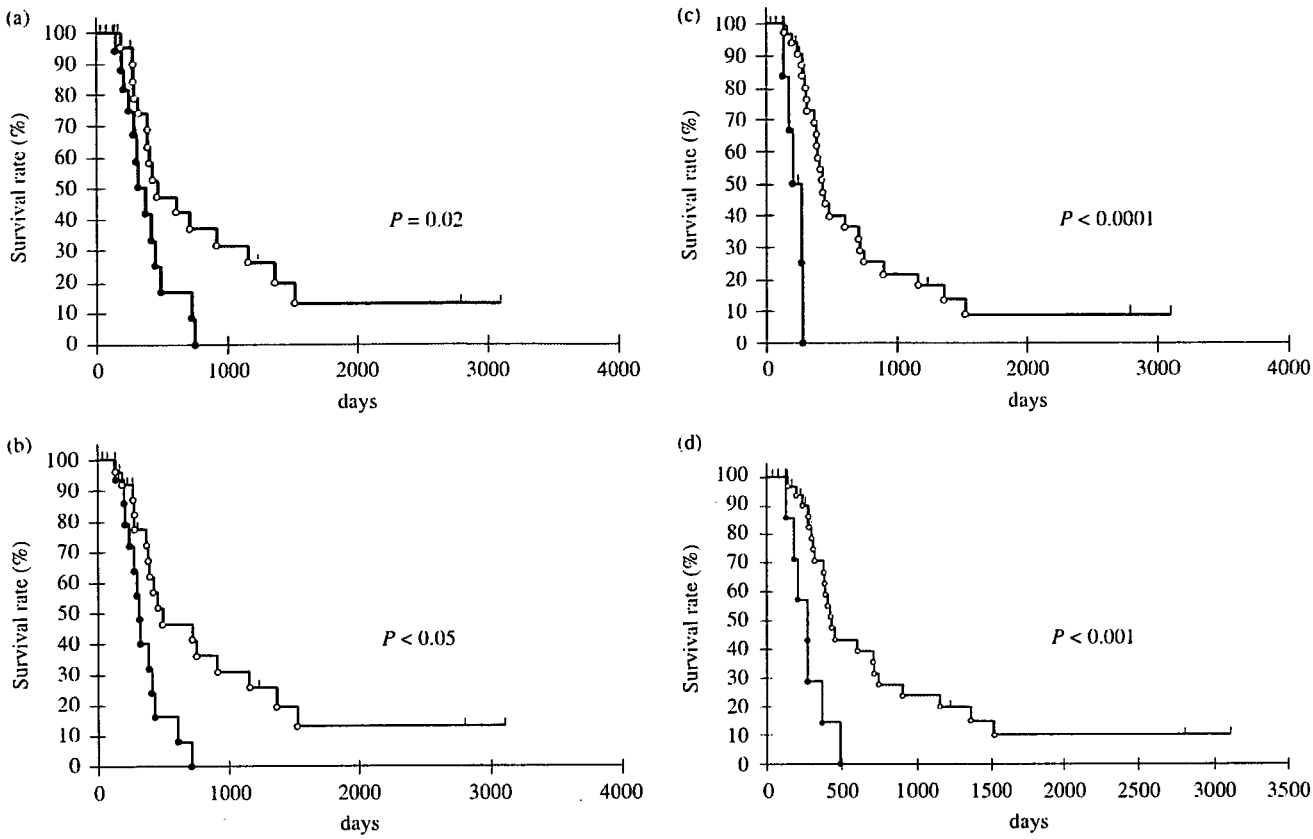

Fig. 3. Overall survival rate of pancreatic cancer patients according to the absence or presence of chromosomal abnormalities. (a) Overall survival rates of cases with chromosomal loss of the p73 locus on 1p36 (indicated as black dots) and cases without such loss (indicated as white dots). (b) Overall survival rates of cases with chromosomal gain of the PPM1D locus on 17q23 (indicated as black dots) and cases without such gain (indicated as white dots). Overall survival rates of cases with chromosomal gain of the (c) LUNX and (d) HCK loci on 20q11 (indicated as black dots) and cases without such gain (indicated as white dots). Survival curves were calculated by the Kaplan–Meier method.

(7q22.1) (Table 5). Genes that were contained in loci frequently amplified but not overexpressed included RBBP8 (18q11.2), LRP1B (2q21.2) and HGF (7q21.1). It should be noted that Smurf1 protein overexpression was also detected in pancreatic cancer clinical samples, as part of a separate study (F. Suzuki, T. Shibata, S. Hirohashi, J. Inazawa, I. Imoto, unpublished data).

The expression levels of genes on 20q11 were examined in more detail, because of the close association of four loci on 20q11 with survival. Eleven genes on 20q11 (BLCAP, RALY, GSS, ID1, NCOA6, TPX2, COX4I2, EPB41L1, BCL2L1, DNCL2A, CTNNBL1) were overexpressed. BCL2L1 (or BCL-x1) expression was also associated with lymph node metastasis of the xenografted tumors in mice (data not shown). It should be noted that two adjacent loci, TNFRSF6B and ZNF217 (20q13), were amplified in three cases each.

Discussion

This study represents the first genome-wide analysis of the subchromosomal numerical aberration profile (here designated SNAP) of a substantial number of pancreatic cancer cases by aCGH and is the first to establish its relationship with particular clinicopathological parameters of known prognostic value. It examined a number of primary tumors large enough to exclude randomly observed alterations from being considered as likely candidates, as would be the case in smaller-scale studies. In all previous studies except one,[29] case selection was based on the exclusion of samples that did not possess a high degree of neoplastic cellularity, which translates to a high copy number ratio error probability. In the present study, tumors were subjected to LCM so as to exclude non-tumor DNA from the analysis and thus increase both the number of available cases and the accuracy of the derived copy number ratio.

One of the striking findings of the study was the wide range in the number and pattern of aberrations observed between cases. Whereas many cases showed few aberrations and two had none whatsoever, 20% of cases showed alterations in more than 50% of loci examined. Importantly, the loss rate and range reported here (17%, 0–46%) is in very close agreement with the one reported in a comprehensive genome-wide allelic loss study of pancreatic cancer (15%, 1.5–32%).[30] It should be noted that it was not possible to know whether alterations of adjacent loci represented single amplicons or losses or whether they were independent events. Our results indicate that in the majority of pancreatic adenocarcinomas genomic instability occurs at the subchromosomal level, affecting a varying but large number of genes, and suggests the presence of multiple or complementary patterns of tumor evolution. Based on the association of SNAP with clinicopathological parameters revealed here, it is fair to assume that some of these aberrations contribute to tumor progression whereas others are the result of it. For the remaining cases showing a low SNAP or absence of aberrations, alternative mechanisms leading to tumor progression may be in place, such as DNA methylation or mismatch repair system aberrations,

doi: 10.1111/j.1349-7006.2007.00395.x

Table 5. Correlation of amplification with overexpression in pancreatic cancer genes both amplified and overexpressed in at least one xenograft

Gene	Locus	Amplified cases (%)	Overexpressed cases (%)	Amplified and overexpressed in the same case (%)	Amplified or gained and overexpressed in the same case (%)
Smurf1	7q22.1	36	25	25	25
BCAS1	20q13.2-q13.3	18	83	17	33
VCL	10q22.1	18	33	17	17
TRRAP	7q22.1	36	17	17	17
SRI	7q21.1	9	83	8	33
Cul3	2q36	27	42	8	33
TPD52	8q21	9	42	8	33
EFNB2	13q33	9	83	8	17
PDAP1	7q22	27	17	8	17
ZNF217	20q13	9	25	8	17
PLAU	10q24	18	17	8	8
WHSC1	4p16.3	9	17	8	8
CDK4	12q14	9	17	8	8
CYP3A4	7q22.1	36	8	8	8
CCNE1	19q11	18	8	8	8
OPG	8q24	9	33	0	33
BARD1	2q34	9	25	0	25
ELE1,MSMB	10q11.2	9	42	0	17
RAP1B	12q14	9	25	0	17
KRAS2	12p12.1	18	17	0	17
DHFR,MSH3	5q11.2-q13.2	9	17	0	17
TPR	1q25	9	17	0	8
MLL5	7q22.3	27	8	0	8
SSXT	18q11.2	27	8	0	8
PEG10	7q21.3	9	8	0	8
NBS1	8q21	9	8	0	8

mutations or small deletions, or chromosomal translocations and rearrangements not accompanied by numerical aberrations. These mechanisms may act in a way complementary to that of numerical aberrations in pancreatic carcinogenesis, so that in cases with high or low SNAP the above-mentioned mechanisms would be expected to play a minor role whereas other alternative mechanisms would be expected to play a minor or major role respectively.

A number of clinicopathological parameters was associated with SNAP, including, importantly, survival probability. Overall, cases with a phenotype indicating increased malignant potential had a higher SNAP. Specific loci, the loss or gain of which is associated with particular clinicopathological characteristics, were identified and are delineated in detail in the results section. Although only a small number of negative tumors was examined, it is noteworthy that loci associated with venous invasion were different from those associated with lymph node metastasis. Our results therefore appear to indicate that invasiveness and metastatic ability result from diverse and distinct molecular mechanisms in pancreatic cancer.

Despite the aforementioned genomic complexity, we identified genes the copy number status of which is associated with survival and may therefore be of prognostic value. Gains of the LUNX (20q11.2), AREG (4q13-q21) and CCNC (6q21) loci were detected exclusively in the short-survival group. Loss of 1p36 (p73) and 11q12-13 was associated with both short-term survival and evidence of venous invasion, whereas gain of 7q21-22 was associated with both short-term survival and the presence of lymph node metastases. Combining the above observations, we identified candidates most likely to yield clinically relevant results. A strong association was revealed between the copy number status of a number of loci at 20q11 and prognosis, mainly concerning the LUNX (PLUNC) locus ($P < 0.0001$) but also including adjacent loci containing HCK, E2F1 and DNMT3b. LUNX is upregulated and has been proposed as a marker for detection of micrometastases in non-small-cell lung cancer.[31] E2F1 activates the transcription of genes that encode proteins necessary for DNA replication, and is deregulated in most tumors.[32] DNMT3b may contribute to tumorigenesis by improper *de novo* methylation and silencing of the promoters of growth-regulatory genes, and its expression may be of clinical significance in breast cancer.[33] Although our data refer to loci rather than individual genes, the significance of the copy aberrations of the above loci has not been described previously in pancreatic or other cancers. Two loci on 20q13 were amplified in three cases each, whereas a further 12 genes on 20q11, including BCL2L1, were overexpressed. BCL2L1 is a BCL2-independent apoptosis regulator located in close proximity to LUNX. Its overexpression has already been linked to short survival times in pancreatic cancer[34,35] and other malignancies, and was also found to be associated with lymph node metastasis in the present study. Amplification and overexpression of BCL10 and BCL6 were also recently described in pancreatic carcinoma.[15] The 11q13.3 locus, containing another BCL family member, BCL1, was found to be amplified frequently in our study, which together with our findings on BCL2L1 described above may indicate a role for the BCL family in pancreatic carcinogenesis. The BCL2L1 overexpression and association with the metastatic phenotype may partially explain the effect the 20q11 region copy number status has on survival. However, we tend to think, in agreement with a similar proposal,[36] that our findings are more indicative of the fact that many (but not all) genes collectively confer selective advantage, in varying degrees of involvement, within the 20q11 region.

Loss of 1p36 (p73) and gain of 17q23 (PPM1D) were also significantly associated with prognosis. As mentioned earlier, 1p36/p73 loss was also associated with evidence of venous invasion in our study. p73, like its homolog p53, is able to induce apoptosis and has been reported to predict clinical outcome

in bladder cancer.[37] PPM1D amplification abrogates p53 tumor-suppressor activity. PPM1D is located within one of the most commonly amplified regions in breast cancer.[38] Gain of 17q21-q24 has also been associated with poor prognosis in ovarian clear cell adenocarcinomas, in which both PPM1D and APPBP2 were identified as likely amplification targets,[39] but, like p73, the PPM1D locus has not been previously reported to be of prognostic significance in pancreatic cancer.

Examination of the association between SNAP and expression provided a satisfactory filter for candidate genes. Only 15 of the 81 loci amplified and 14.7% (20/136) of individual amplifications observed contained genes that were overexpressed concurrently. This concordance level lies between those observed in breast cancer[40,41] and colon cancer,[42] in which 44–62% and 4%, respectively, of genes showing amplifications were overexpressed. It is, however, significantly lower than the one recently reported for pancreatic cancer cell lines, in which 60% of the genes within highly amplified genomic regions displayed associated overexpression,[14] a discrepancy that may partially be explained by the different source used (primary tumors vs cell lines) and the fact that we examined loci rather than genes. More than one target gene was overexpressed in some amplicons in our study, a finding not in disagreement with the above study.[14] We identified four genes contained in loci that were amplified and that were overexpressed recurrently: Smurf1 and TRRAP, both at 7q22.1, BCAS1 (20q13.2-3), and VCL (10q22.1). Smurf1 acts as a negative regulator of transfroming growth factor β signaling.[43] It was amplified in six cases overall and overexpressed concurrently in four. Although, as mentioned, gain of the Smurf1 locus was not associated with poor prognosis, 7q21-22 gain was associated with the presence of lymph node metastasis and was detected significantly more frequently in the short-term (<3 years) survival group. TRRAP is an essential cofactor for both the c-Myc and E1A/E2F oncogenic transcription factor pathways and interacts specifically with the E2F-1 transactivation domain. Its inclusion among the four genes both amplified and overexpressed lends further support to the association between E2F1 gain and poor survival revealed here. The fact that Smurf1 and TRRAP are amplified in pancreatic cancer was reported recently, albeit only in cell lines.[16] We show that amplifications of these genes also occurs in primary tumors and that they are recurrently accompanied by overexpression, therefore presenting as very likely novel oncogenes in pancreatic cancer. BCAS1 (20q13), reported to be amplified and overexpressed in breast cancer,[44] was the most frequently overexpressed gene among the ones contained in loci recurrently amplified, and may therefore have a similar role in pancreatic cancer; 20q13 was also one of the most frequently amplified loci in a recent aCGH study on pancreatic cancer.[14,15] Finally, 10q22-24 contained another novel candidate, vinculin, an intracellular protein with a crucial role in the maintenance and regulation of cell adhesion and migration.[45] KRAS2 and 20 other genes have recently been identified as potential target genes on 12p.[36] This finding is in partial agreement with our study, in which five loci on 12p were amplified and KRAS2 was amplified in two cases.

Numerous recurrent, non-random, patterns of subchromosomal aberrations have emerged through our analysis. Thirty-three loci with frequent losses (>50% cases) were identified. The chromosome arms found to contain the highest number of loci lost are in agreement with allelic loss[30] and chromosome CGH studies, with the additional detection of losses at 5p, 8q, 9q, 11p, 16p and 20q. The most frequently lost loci were: 17p13.3 (in 75% of cases), containing ABR, a multifunctional cellular signaling regulator and a putative TSG in medulloblastoma, 18qtel (CTDP1, SHGC-145820, 68%) and 18q21 (66%), containing SMAD7, a member of the SMAD family, although all three are close to either the p53 or the DPC4 locus. HD were detected in 25% of cases, affecting 26 loci. The 1p353-6.33 region contained the highest number of loci deleted (six) or lost (16). The most frequently deleted locus was 9p21 spanning the p16 gene, the inactivation of which is known to play an established role in pancreatic carcinogenesis. The above regions (17p, 18q and 1p353-6) have been reported previously to show frequent loss.[19] The most frequently gained locus was 7q21.1 (71%) containing the HGF gene, which encodes a cytokine involved in initiating cell migration. Some regions in which gains were observed frequently, at 6p21 (2 loci), 11q22 (7 loci) 12p12 (three loci) and 17q12 (Suppl. Table 4), have been previously proposed as novel amplicons.[16] Sixteen loci were amplified frequently (>10%), although, again, the possibility of another gene being amplified within these loci cannot be excluded. Two of the most frequently amplified loci were on 11q13, in agreement with a report by Holzmann *et al.* on 13 pancreatic cancer cell lines and six primary tumors.[15]

Novel loci likely to play important roles in pancreatic carcinogenesis and in the acquisition of certain malignant phenotypes were identified. Genes associated with prognosis or established histopathological indicators of malignancy, or showing both numerical aberrations and overexpression, may represent novel oncogenes. The copy number alterations of the p73 and PPM1D loci, the 20q11 region, including LUNX, and the loci amplified that contained genes concurrently overexpressed, particularly Smurf1, shown here may be of great importance for predicting clinical outcomes and setting new therapeutic targets in pancreatic cancer but will require prospective studies in order to be firmly established.

Acknowledgments

We thank T. Sakiyama for helping with the aCGH data analysis, T. Kondo for advice on statistical analysis, and Y. Arai, S. Uryu and Y. Kuwabara for advice on the hybridization technique. This study was supported in part by a Grant-in-Aid for the Second Term Comprehensive 10-Year Strategy for Cancer Control from the Ministry of Health, Labor and Welfare of Japan; the Program for Promotion of Fundamental Studies in Health Sciences of the National Institute of Biomedical Innovation (NiBio), Japan; and by a Grant-in-Aid from CREST of JST. P. L. was a recipient of a Research Fellowship from the Program for Invitation of Foreign Researchers from the Foundation for Promotion of Cancer Research in Japan. H. K. was a recipient of a Research Resident Fellowship from the Foundation for Promotion of Cancer Research.

References

1 Conlon KC, Klimstra DS, Brennan MF. Long-term survival after curative resection for pancreatic ductal adenocarcinoma. Clinicopathologic analysis of 5-year survivors. *Ann Surg* 1996; **223**: 273–9.
2 Torrisani J, Buscail L. Molecular pathways of pancreatic carcinogenesis. *Ann Pathol* 2002; **22**: 349–55.
3 Kallioniemi A, Kallioniemi OP, Sudar D *et al.* Comparative genomic hybridization for molecular cytogenetic analysis of solid tumors. *Science* 1992; **258**: 818–21.
4 Johansson B, Bardi G, Heim S *et al.* Nonrandom chromosomal rearrangements in pancreatic carcinomas. *Cancer* 1992; **69**: 1674–81.
5 Bardi G, Johansson B, Pandis N *et al.* Karyotypic abnormalities in tumours of the pancreas. *Br J Cancer* 1993; **67**: 1106–12.
6 Hahn SA, Seymour AB, Hoque AT *et al.* Allelotype of pancreatic adenocarcinoma using xenograft enrichment. *Cancer Res* 1995; **55**: 4670–5.
7 Armengol G, Knuutila S, Lluis F, Capella G, Miro R, Caballin MR. DNA copy number changes and evaluation of MYC, IGF1R, and FES amplification in xenografts of pancreatic adenocarcinoma. *Cancer Genet Cytogenet* 2000; **116**: 133–41.
8 Griffin CA, Hruban RH, Morsberger LA *et al.* Consistent chromosome abnormalities in adenocarcinoma of the pancreas. *Cancer Res* 1995; **55**: 2394–9.
9 Mahlamaki EH, Hoglund M, Gorunova L *et al.* Comparative genomic hybridization reveals frequent gains of 20q, 8q, 11q, 12p, and 17q, and losses

doi: 10.1111/j.1349-7006.2007.00395.x

of 18q, 9p, and 15q in pancreatic cancer. *Genes Chromosomes Cancer* 1997; **20**: 383–91.
10 Schleger C, Arens N, Zentgraf H, Bleyl U, Verbeke C. Identification of frequent chromosomal aberrations in ductal adenocarcinoma of the pancreas by comparative genomic hybridization (CGH). *J Pathol* 2000; **191**: 27–32.
11 Heidenblad M, Jonson T, Mahlamaki EH *et al.* Detailed genomic mapping and expression analyses of 12p amplifications in pancreatic carcinomas reveal a 3.5-Mb target region for amplification. *Genes Chromosomes Cancer* 2002; **34**: 211–23.
12 Gorunova L, Hoglund M, Andren-Sandberg A *et al.* Cytogenetic analysis of pancreatic carcinomas: intratumor heterogeneity and nonrandom pattern of chromosome aberrations. *Genes Chromosomes Cancer* 1998; **23**: 81–99.
13 Heidenblad M, Schoenmakers EF, Jonson T *et al.* Genome-wide array-based comparative genomic hybridization reveals multiple amplification targets and novel homozygous deletions in pancreatic carcinoma cell lines. *Cancer Res* 2004; **64**: 3052–9.
14 Aguirre AJ, Brennan C, Bailey G *et al.* High-resolution characterization of the pancreatic adenocarcinoma genome. *Proc Natl Acad Sci USA* 2004; **101**: 9067–72.
15 Holzmann K, Kohlhammer H, Schwaenen C *et al.* Genomic DNA-chip hybridization reveals a higher incidence of genomic amplifications in pancreatic cancer than conventional comparative genomic hybridization and leads to the identification of novel candidate genes. *Cancer Res* 2004; **64**: 4428–33.
16 Bashyam MD, Bair R, Kim YH *et al.* Array-based comparative genomic hybridization identifies localized DNA amplifications and homozygous deletions in pancreatic cancer. *Neoplasia* 2005; **7**: 556–62.
17 Gysin S, Rickert P, Kastury K, McMahon M. Analysis of genomic DNA alterations and mRNA expression patterns in a panel of human pancreatic cancer cell lines. *Genes Chromosomes Cancer* 2005; **44**: 37–51.
18 Mahlamaki EH, Kauraniemi P, Monni O, Wolf M, Hautaniemi S, Kallioniemi A. High-resolution genomic and expression profiling reveals 105 putative amplification target genes in pancreatic cancer. *Neoplasia* 2004; **6**: 432–9.
19 Nowak NJ, Gaile D, Conroy JM *et al.* Genome-wide aberrations in pancreatic adenocarcinoma. *Cancer Genet Cytogenet* 2005; **161**: 36–50.
20 Loukopoulos P, Kanetaka K, Takamura M, Shibata T, Sakamoto M, Hirohashi S. Orthotopic transplantation models of pancreatic adenocarcinoma derived from cell lines and primary tumors and displaying varying metastatic activity. *Pancreas* 2004; **29**: 193–203.
21 Japan Pancreas Society. *Classification of Pancreatic Carcinoma*, 2nd English edn. Tokyo: Kanehara and Co., 2003.
22 Tanabe C, Aoyagi K, Sakiyama T *et al.* Evaluation of a whole-genome amplification method based on adaptor-ligation PCR of randomly sheared genomic DNA. *Genes Chromosomes Cancer* 2003; **38**: 168–76.
23 Sonoda I, Imoto I, Inoue J *et al.* Frequent silencing of low density lipoprotein receptor-related protein 1B (LRP1B) expression by genetic and epigenetic mechanisms in esophageal squamous cell carcinoma. *Cancer Res* 2004; **64**: 3741–7.
24 Takada H, Imoto I, Tsuda H *et al.* Screening of DNA copy-number aberrations in gastric cancer cell lines by array-based comparative genomic hybridization. *Cancer Sci* 2005; **96**: 100–10.
25 Peng W-X, Shibata T, Katoh H *et al.* Array-based comparative genomic hybridization analysis of high-grade neuroendocrine tumors of the lung. *Cancer Sci* 2005; **96**: 661–7.
26 Katoh H, Shibata T, Kokubu A *et al.* Genetic profile of hepatocellular carcinoma revealed by array-based comparative genomic hybridization: Identification of genetic indicators to predict patient outcome. *J Hepatol* 2005; **43**: 863–74.
27 Yamazaki K, Sakamoto M, Ohta T, Kanai Y, Ohki M, Hirohashi S. Overexpression of KIT in chromophobe renal cell carcinoma. *Oncogene* 2003; **22**: 847–52.
28 Tanno S, Mitsuuchi Y, Altomare DA, Xiao GH, Testa JR. AKT activation up-regulates insulin-like growth factor I receptor expression and promotes invasiveness of human pancreatic cancer cells. *Cancer Res* 2001; **61**: 589–93.
29 Kitoh H, Ryozawa S, Harada T *et al.* Comparative genomic hybridization analysis for pancreatic cancer specimens obtained by endoscopic ultrasonography-guided fine-needle aspiration. *J Gastroenterol* 2005; **40**: 511–17.
30 Iacobuzio-Donahue CA, van der Heijden MS, Baumgartner MR *et al.* Large-scale allelotype of pancreaticobiliary carcinoma provides quantitative estimates of genome-wide allelic loss. *Cancer Res* 2004; **64**: 871–5.
31 Iwao K, Watanabe T, Fujiwara Y *et al.* Isolation of a novel human lung-specific gene, LUNX, a potential molecular marker for detection of micrometastasis in non-small-cell lung cancer. *Int J Cancer* 2001; **91**: 433–7.
32 Phillips AC, Ernst MK, Bates S, Rice NR, Vousden KH. E2F-1 potentiates cell death by blocking antiapoptotic signaling pathways. *Mol Cell* 1999; **4**: 771–81.
33 Girault I, Tozlu S, Lidereau R, Bieche I. Expression analysis of DNA methyltransferases 1, 3A, and 3B in sporadic breast carcinomas. *Clin Cancer Res* 2003; **9**: 4415–22.
34 Friess H, Lu Z, Andren-Sandberg A *et al.* Moderate activation of the apoptosis inhibitor bcl-xL worsens the prognosis in pancreatic cancer. *Ann Surg* 1998; **228**: 780–7.
35 Ghaneh P, Kawesha A, Evans JD, Neoptolemos JP. Molecular prognostic markers in pancreatic cancer. *J Hepatobiliary Pancreat Surg* 2002; **9**: 1–11.
36 Heidenblad M, Lindgren D, Veltman JA *et al.* Microarray analyses reveal strong influence of DNA copy number alterations on the transcriptional patterns in pancreatic cancer: implications for the interpretation of genomic amplifications. *Oncogene* 2005; **24**: 1794–801.
37 Matsumoto H, Matsuyama H, Fukunaga K, Yoshihiro S, Wada T, Naito K. Allelic imbalance at 1p36 may predict prognosis of chemoradiation therapy for bladder preservation in patients with invasive bladder cancer. *Br J Cancer* 2004; **91**: 1025–31.
38 Li J, Yang Y, Peng Y *et al.* Oncogenic properties of PPM1D located within a breast cancer amplification epicenter at 17q23. *Nat Genet* 2002; **31**: 133–4.
39 Hirasawa A, Saito-Ohara F, Inoue J *et al.* Association of 17q21-q24 gain in ovarian clear cell adenocarcinomas with poor prognosis and identification of PPM1D and APPBP2 as likely amplification targets. *Clin Cancer Res* 2003; **9**: 1995–2004.
40 Hyman E, Kauraniemi P, Hautaniemi S *et al.* Impact of DNA amplification on gene expression patterns in breast cancer. *Cancer Res* 2002; **62**: 6240–5.
41 Pollack JR, Sorlie T, Perou CM *et al.* Microarray analysis reveals a major direct role of DNA copy number alteration in the transcriptional program of human breast tumors. *Proc Natl Acad Sci USA* 2002; **99**: 12 963–8.
42 Platzer P, Upender MB, Wilson K *et al.* Silence of chromosomal amplifications in colon cancer. *Cancer Res* 2002; **62**: 1134–8.
43 Zhu H, Kavsak P, Abdollah S, Wrana JL, Thomsen GH. A SMAD ubiquitin ligase targets the BMP pathway and affects embryonic pattern formation. *Nature* 1999; **400**: 687–93.
44 Collins C, Rommens JM, Kowbel D *et al.* Positional cloning of ZNF217 and NABC1: genes amplified at 20q13.2 and overexpressed in breast carcinoma. *Proc Natl Acad Sci USA* 1998; **95**: 8703–8.
45 Bakolitsa C, Cohen DM, Bankston LA *et al.* Structural basis for vinculin activation at sites of cell adhesion. *Nature* 2004; **430**: 583–6.

Supplementary material

This material is available as part of the online article from:

The following supplementary material is available for this article:

Fig. S1. Homozygous deletions detected by array-based comparative genomic hybridization were validated by polymerase chain reaction and gel electrophoresis for selected cases and genes. Genes contained in the two most frequently deleted loci, p16 (left panel gel, cases 12, 18 and 41) at 9p21 and ABCA3 (right panel gel, cases 44 and 47) at 16p13.3 were examined (exons 2 and 28, respectively). Homozygous deletions were confirmed in all five cases examined, whereas wild-type products were detected in all control tissues used. The control tissue for p16 consisted of the corresponding normal tissue in one of three cases examined; corresponding normal tissue was not available for the other two cases (cases 12 and 18) as they derived from xenografts. The control tissues for the cases examined for homozygous deletions of the ABCA3 gene consisted of: (a) the corresponding normal tissues of both cases and (b) a third case (case no. 40), in which the array-based comparative genomic hybridization signal ratio indicated loss of heterozygosity of the ABCA3 gene, but not homozygous deletion, and its corresponding normal tissue.

Fig. S2. Range of numerical aberrations observed between cases. The total number of (a) numerical aberrations, (b) losses and (c) gains observed ranged widely between cases. In two cases no copy number changes were observed (a–c), whereas nine cases (20%) had alterations in more than 50% of loci (>400 loci) (a). Although the loss range was wider than the gain range (b,c), in most cases the number of gains was higher than the number of losses. Overall, however, the loss rate was similar to the gain rate (19% of loci altered on average per case for both).

Table S1 Clinicopathological parameters of 43 pancreatic cancer cases analyzed by array-based comparative genomic hybridization.

Table S2 Numerical aberrations observed in 44 pancreatic adenocarcinoma cases examined by array-based comparative genomic hybridization.

Table S3 Loci lost frequently (>25% cases) in 44 pancreatic adenocarcinoma cases examined by array-based comparative genomic hybridization, arranged by region.

Table S4 Loci gained frequently (>25% cases) in 44 pancreatic adenocarcinoma cases examined by array-based comparative genomic hybridization, arranged by region.

Table S5 Association of sub-chromosomal numerical aberrations with selected clinicopathological parameters in pancreatic cancer.

Table S6 (A) Loci altered more frequently in moderately compared with well differentiated pancreatic adenocarcinomas. (B) Loci altered more frequently in poorly compared with moderately differentiated pancreatic adenocarcinomas.

http://www.blackwell-synergy.com/doi/abs/10.1111/j.1349-7006.2006.00395.x

(This link will take you to the article abstract).

Please note: Blackwell Publishing are not responsible for the content or functionality of any supplementary materials supplied by the authors. Any queries (other than missing material) should be directed to the corresponding author for the article.

doi: 10.1111/j.1349-7006.2007.00395.x

FOXP3$^+$ Regulatory T Cells Affect the Development and Progression of Hepatocarcinogenesis

Noritoshi Kobayashi,[1] Nobuyoshi Hiraoka,[1] Wataru Yamagami,[1] Hidenori Ojima,[1] Yae Kanai,[1] Tomoo Kosuge,[2] Atsushi Nakajima,[3] and Setsuo Hirohashi[1]

Abstract **Purpose:** Tumor-infiltrating lymphocytes represent the host immune response to cancer. CD4$^+$CD25$^+$FOXP3$^+$ regulatory T cells (Tregs) suppress the immune reaction. The aim of the present study was to investigate the clinicopathologic significance and roles of Tregs and CD8$^+$ T cells during hepatocarcinogenesis.

Experimental Design: We examined the infiltration of FOXP3$^+$ Tregs and CD8$^+$ T cells in the tumor stroma and nontumorous liver parenchyma using 323 hepatic nodules including precursor lesions, early hepatocellular carcinoma (HCC), and advanced HCC, along with 39 intrahepatic cholangiocarcinomas and 59 metastatic liver adenocarcinomas. We did immunohistochemical comparative studies.

Results: The prevalence of Tregs was significantly higher in HCC than in the nontumorous liver ($P < 0.001$). The patient group with a high prevalence of Tregs infiltrating HCC showed a significantly lower survival rate ($P = 0.007$). Multivariate analysis revealed that the prevalence of Tregs infiltrating HCC was an independent prognostic factor. The prevalence of Tregs increased in a stepwise manner ($P < 0.001$) and that of CD8$^+$ T cells decreased during the progression of hepatocarcinogenesis ($P < 0.001$). Regardless of the presence of hepatitis virus infection or histopathologic evidence of hepatitis, the prevalence of Tregs was significantly increased in nontumorous liver bearing primary hepatic tumors.

Conclusions: Tregs play a role in controlling the immune response to HCC during the progression of hepatocarcinogenesis. It has been suggested that primary hepatic cancers develop in liver that is immunosuppressed by a marked infiltration of Tregs. A high prevalence of Tregs infiltrating HCC is thought to be an unfavorable prognostic indicator.

Hepatocellular carcinoma (HCC) is the fifth most common cancer in the world, representing the third most common cause of mortality among deaths from cancer (1). Even with remarkable advances in diagnostic and therapeutic techniques, the incidence of HCC is still on the increase. Hepatitis virus B (HBV) and hepatitis virus C (HCV) are known to be major risk factors, and chronic infection with these viruses is responsible for ~80% of HCCs in humans (2). Most of the HCCs occur in damaged liver (chronic hepatitis or liver cirrhosis), even if the liver is not infected with HBV or HCV (3). HCC is also characterized by an obvious multistage process of tumor progression (4–7), from a regenerative nodule to adenomatous hyperplasia (AH), and thereafter to atypical adenomatous hyperplasia (AAH), early HCC (defined as *in situ* or microinvasive cancer), and advanced HCC. It is important to detect cancers at an early stage, including their precursor lesions, and to assess their risk in order to provide appropriate treatment and reduce cancer-related mortality.

Previous studies have investigated the changes in morphology, genetics, and molecular biology of epithelial cells during tumorigenesis. Recently, many studies have suggested that the tumor microenvironment also plays an important role in the establishment and progression of tumors. Lymphocytes contribute to the tumor microenvironment through immunity and inflammation. CD8$^+$ CTLs can directly kill target cells by releasing granules including membrane-lytic materials such as perforin and granzymes in acquired immune responses, thereby playing a central role in antitumor immunity. Indeed, a high frequency of CD8$^+$ T cells infiltrating cancer tissue can be a favorable prognostic indicator in ovarian cancer (8) and colorectal cancer (9). In HCC, extremely marked infiltration of T cells including predominant CD8$^+$ T cells has been shown to be closely associated with a low recurrence rate and good prognosis (10). On the other hand, another study using a mouse model has

Authors' Affiliations: [1]Pathology Division, National Cancer Center Research Institute; [2]Division of Hepato-Biliary and Pancreatic Surgery, National Cancer Center Hospital, Tokyo, Japan; and [3]Gastroenterology Division, Yokohama City University Hospital, Yokohama, Japan

Received 9/25/06; revised 10/29/06; accepted 11/8/06.

Grant support: Grant-in-Aid for Third Term Comprehensive 10-year Strategy for Cancer Control from the Ministry of Health, Labor, and Welfare of Japan and a Grant-in-Aid for Scientific Research from the Ministry of Education, Culture, Sports, Science, and Technology of Japan. N. Kobayashi and W. Yamagami are recipients of a Research Resident Fellowship from the Foundation for Promotion of Cancer Research in Japan.

The costs of publication of this article were defrayed in part by the payment of page charges. This article must therefore be hereby marked *advertisement* in accordance with 18 U.S.C. Section 1734 solely to indicate this fact.

Requests for reprints: Nobuyoshi Hiraoka, Pathology Division, National Cancer Center Research Institute, 5-1-1 Tsukiji, Chuo-ku, Tokyo 104-0045, Japan. Phone: 81-33542-2511; Fax: 81-33248-2463; E-mail: nhiraoka@gan2.res.ncc.go.jp.

doi:10.1158/1078-0432.CCR-06-2363

shown that marked infiltration of $CD8^+$ T cells exacerbates liver damage, thus accelerating the development of HCC (11).

In contrast to $CD8^+$ CTL, which generally exert a suppressive influence on tumor growth, regulatory T cells (Tregs) are thought to have a positive effect on tumor growth through suppression of antitumor immune cells. $CD4^+CD25^+$ Tregs are a minor but functionally unique population of T cells, which maintain immune homeostasis in immune tolerance and the control of autoimmunity. Tregs can inhibit immune responses mediated by $CD4^+CD25^-$ and $CD8^+$ T cells *in vitro* by a contact-dependent and cytokine-independent mechanism (12–14), although more recent reports suggest that the immune suppression mechanisms of Tregs *in vivo* are more complex (15, 16). Forkhead or winged helix family of transcription factor P3 (FOXP3) is critical for the development and function of Tregs in mice and humans (16, 17), and is still the only marker for evaluating real Tregs that have a suppressive function. In murine models, it has been described that Tregs inhibit the antitumor immune response (15, 18–20). Involvement of $CD4^+CD25^+$ Tregs in human cancer has been observed in peripheral blood and tumor tissues from patients with several types of cancer (21–25). A few groups have reported that Tregs are increased in peripheral blood and among tumor-infiltrating lymphocytes of patients with HCC (26–28), although these were not large-scale studies and did not estimate the clinicopathologic significance of Tregs infiltrating HCC, including their prognostic value. Early studies detected Tregs not as $FOXP3^+$ T cells but as $CD4^+CD25^+$ T cells, although recent studies have revealed that $CD4^+CD25^+$ T cells consist of Tregs and activated effector T cells, the latter being increased in inflammatory lesions (29). Furthermore, no previous study has investigated host immune responses in multistage hepatocarcinogenesis.

In the present study, we first investigated the clinicopathologic values of both $FOXP3^+$ Tregs and $CD8^+$ T cells infiltrating the tumor stroma of HCC, and then examined the prevalence of $FOXP3^+$ Tregs and $CD8^+$ T cells during multistage hepatocarcinogenesis. Precursor lesions of HCC are small nodular lesions that can be detected and evaluated only by microscopic analysis, making it difficult to extract living immune cells from them and to analyze their immunophenotypes and immune functions. Therefore, we selected an immunohistochemical comparative approach for evaluating host immune responses in these HCC precursor lesions. This approach was used in the other experiments as well. We also investigated whether Tregs are involved in the development of HCC, and compared the host immune responses by measuring and comparing the infiltration of Tregs and $CD8^+$ T cells between HCC and primary hepatic adenocarcinoma, intrahepatic cholangiocarcinoma (ICC) as well as between primary and metastatic liver tumors. We compared the prevalence of Tregs in nontumorous liver parenchyma among patients with and without primary hepatic tumors, and those with and without hepatitis viral infection. The results showed that the prevalence of Tregs increases during the progression of established cancers as well as that of their precursor lesions. Furthermore, the prevalence of Tregs was significantly correlated with patient survival, independent of other prognostic factors.

Materials and Methods

Patients and samples. This study was approved by the Ethics Committee of the National Cancer Center, Tokyo, Japan. Clinical and pathologic data and the specimens used for immunohistochemical analysis were obtained through a detailed retrospective review of the medical records of 218 patients with 323 hepatic nodules of HCC or its precursor lesions who had undergone initial surgical resection between 1992 and 2000 at the National Cancer Center Hospital, Tokyo, Japan. None of the nodules had been treated previously with techniques such as radiofrequency ablation, percutaneous ethanol injection therapy, or transcatheter arterial embolization or injection, and none of the patients with nodules had received systemic chemotherapy. Sixty-five patients had hepatic cancers that had been treated by surgical resection, radiofrequency ablation, percutaneous ethanol injection therapy, or transcatheter arterial embolization or injection; the current nodules were also located in different lobes, as well as distant from, the previous cancers. In another six patients, curative resection was not done. The remaining 147 patients were studied in order to evaluate the clinicopathologic correlation of the prevalence of $FOXP3^+$ Tregs and $CD8^+$ T cells with specific variables. Tumors were classified according to the WHO classification (30) and the International Union against Cancer tumor-node-metastasis (TNM) classification (31). If patients had multiple nodules in the liver, we selected the nodule showing the most advanced histologic grade for our study. If a tumor had different grades of histology, the grade of the tumor was regarded as the most advanced one among them. Nontumorous liver was classified histopathologically into four categories: non-chronic hepatitis (NCH), chronic hepatitis (CH), chronic hepatitis with cirrhotic change (pre-cirrhotic stage; PC), and liver cirrhosis (LC), which corresponded to 0, 1-3, 4-5, and 6 of the fibrosis stages of the modified histological activity index system (32). There were 5 patients with HBV infection and 15 patients without HBV or HCV infection in NCH, which included liver with fatty changes and/or slight inflammatory infiltrates in the portal area. All patients had complete medical records and had been followed by the tumor registries for survival and outcome. Follow-up was available in all cases and ranged from 0.5 to 169.1 months (mean, 52.8 months). The latest survival data were collected on April 30, 2006. The overall survival rate at 5 years and the disease-free survival rate were 39.5% and 18.4%, respectively. The clinicopathologic features of the patients are summarized in Table 1.

We also investigated 39 patients with ICC and 59 patients with metastatic liver tumors from primary colorectal cancer who had undergone initial surgical resection between 1991 and 2005 at the National Cancer Center Hospital. The patients with ICC or metastatic liver cancer without hepatitis viral infection were randomly selected and those with hepatitis viral infection were all the patients we had. The patients with ICC comprised 22 males and 17 females, and their median age at surgery was 63 years (range, 44-85 years). HBV and HCV infection were detected in four and five patients, respectively. Their livers were diagnosed histopathologically as CH in eight patients and as PC in one patient. NCH were found in the liver of 30 patients without any HBV or HCV infection. Tumor diameters ranged from 15 to 140 mm (mean, 64.6 ± 30.6 mm). There were 8 patients at stage I, 9 patients at stage II, 3 patients at stage IIIa, 7 patients at stage IIIb, and 12 patients at stage IIIc according to the International Union against Cancer staging classification (31). ICCs were classified histopathologically as well-differentiated adenocarcinoma in 7 cases, moderately differentiated adenocarcinoma in 27, and poorly differentiated adenocarcinoma in 5 according to the WHO classification (30). The patients with liver metastasis from colorectal cancer comprised 37 males and 22 females, and their median age at surgery was 62 years (range, 34-81 years). HBV and HCV virus infection were detected in 8 and 21 patients, respectively, and their livers were diagnosed histopathologically as CH in 18 and as NCH in 11. The other 30 patients had not been infected with HBV or HCV and their nontumorous liver showed no inflammatory or fatty changes. Therefore, the nontumorous liver tissue from these patients was defined as "healthy liver." Thirty-three patients had a solitary tumor and 26 had multiple tumors. Tumor diameters ranged from 12 to 150 mm

Table 1. Clinicopathologic features of the patients

Variables	Results
Characteristics of the patients with HCC (218 cases)	
Age, y (median, range)	62, 17-84
Gender (male/female)	170/48
Virus infection [HBV/HCV/HBV+HCV/(−)]	57/117/10/34
Nontumor liver (NCH/CH/PC/LC)	20/101/35/62
Tumor nodules (AH/AAH/early HCC/WD HCC/MD HCC/PD HCC)	11/9/68/58/123/54
Clinicopathologic findings of the patients with HCC (147 cases)	
Age, y (median, range)	62, 17-83
Gender (male/female)	113/34
Virus infection [HBV/HCV/HBV+HCV/(−)]	47/79/9/12
Nontumor liver (NCH/CH/PC/LC)	17/71/23/36
Child-Pugh classification (A/B/C)	136/11/0
TNM stage (I/II/III/IV)	57/53/37/0
Histologic grade (early HCC/WD HCC/MD HCC/PD HCC)	17/15/77/38
AFP, ng/mL (median, range)	27.1, 1-27,170
VP (presence/absence)	57/90
IM (presence/absence)	33/114
Tumor size, mm (median, range)	35, 6-185

Abbreviations: MD, moderately differentiated; PD, poorly differentiated; WD, well differentiated.

(mean, 42.3 ± 28.2 mm). Histopathologically, the tumors were well-differentiated adenocarcinoma in 5 cases, moderately differentiated adenocarcinoma in 53 cases, and poorly differentiated adenocarcinoma in 1 case.

Immunohistochemical analysis. Immunohistochemistry was done on the formalin-fixed, paraffin-embedded tissue sections as described previously (33). We reacted 4-μm-thick sections of representative blocks with monoclonal antibodies against the following: CD4 (1F6; 1:50), CD8 (4B11; 1:50), and perforin (5B11; 1:50) from Novocastra Laboratories, Ltd. (Newcastle upon Tyne, United Kingdom), and FOXP3 (clone 42; ref. 25). Briefly, the sections were deparaffinized and rehydrated. After blocking of endogenous peroxidase with methanol containing 0.3% H_2O_2, the sections were autoclaved at 121°C for 10 min in citrate buffer (10 mmol/L sodium citrate; pH 6.0) for antigen retrieval. After blocking with normal goat serum, the sections were reacted overnight with appropriately diluted primary antibodies. The sections were then reacted sequentially with biotin-conjugated anti-mouse IgG antibodies (Vector Laboratories, Burlingame, CA) and Vectastain Elite ABC reagent (Vector Laboratories). For staining CD4 and CD8, a CSA system (DAKO, Glöstrup, Denmark) and EnVision$^+$ Polymer system (DAKO) were used, respectively, instead of the avidin-biotin complex system. Diaminobenzidine was used as the chromogen, and the nuclei were counterstained with hematoxylin.

Serial sections were prepared from each paraffin block. The first section was stained with H&E and the second, third, and fourth sections were subjected to immunohistochemistry to detect the CD8, CD4, and FOXP3 antigens. CD8$^+$, CD4$^+$, or FOXP3$^+$ lymphocytes were counted in the corresponding visual fields. Quantitative evaluation of lymphocytes was done by analyzing at least three different high-power fields (×40 objective and ×10 eyepiece). The proportion of FOXP3$^+$ lymphocytes among CD4$^+$ lymphocytes and that of CD8$^+$ lymphocytes among total T cells, together with the sum of CD4$^+$ and CD8$^+$ lymphocytes, were calculated for each field and the averages were compared.

Statistical analysis. Values were expressed as mean ± SD. Statistical analyses were done with StatView-J 5.0 software (Abacus Concepts, Berkeley, CA). Associations among the variables were assessed by the χ^2 test, Student's t test, Mann-Whitney U test, and Kruskal-Wallis test. If there was evidence of non-normality, the Mann-Whitney U test or the Kruskal-Wallis test was used to test the difference in medians among the groups. Survival rates were calculated by the Kaplan-Meier method. Differences between survival curves were analyzed by the log-rank test. To assess the correlation between survival time and multiple clinicopathologic variables, multivariate analyses were done by the Cox proportional hazards regression model. Differences were considered significant at $P < 0.05$.

Results

Increased populations of FOXP3$^+$ Tregs among CD4$^+$ T cells in tumor stroma of HCC. In order to assess the infiltration of Tregs in the stroma of HCC (n = 235) and nontumorous liver (n = 248), we evaluated both the absolute numbers of FOXP3$^+$ Tregs and the prevalence of FOXP3$^+$ Tregs among CD4$^+$ T cells. The absolute number of FOXP3$^+$ Tregs that had infiltrated HCC was significantly higher than that of Tregs in nontumorous liver from patients with HCC or healthy liver tissue (versus healthy controls, $P < 0.001$; versus NCH, $P < 0.001$; versus CH, $P = 0.002$; versus PC, $P = 0.023$; versus LC, $P < 0.001$; Fig. 1A). The prevalence of tumor-infiltrating FOXP3$^+$ Tregs among CD4$^+$ T cells in HCC was also significantly higher (versus healthy controls, $P < 0.001$; versus NCH, $P < 0.001$; versus CH, $P < 0.001$; versus PC, $P < 0.001$; versus LC, $P < 0.001$; Fig. 1B). Among advanced HCCs, the prevalence of FOXP3$^+$ Tregs was significantly higher in less differentiated HCCs (Kruskal-Wallis test, $P < 0.001$; Fig. 1B). No significant difference in the infiltration of Tregs was found among CH, PC, and LC. The prevalence of Tregs in NCH was lower than that in CH ($P = 0.021$), PC, and LC, but was significantly higher than that in healthy controls ($P < 0.001$; Fig. 1B).

The absolute number of CD8$^+$ T cells was increased in CH, PC, and LC, and was significantly higher than that in HCC ($P < 0.001$; Fig. 1C). The prevalence of CD8$^+$ T cells in HCC was significantly lower than that in any type of damaged and nontumorous liver from patients with HCC (versus NCH, $P = 0.025$; versus CH, $P < 0.001$; versus PC, $P = 0.015$; versus LC, $P < 0.001$; Fig. 1D). In advanced HCCs, the prevalence of CD8$^+$ T cells was significantly lower in less differentiated HCC (Kruskal-Wallis test, $P = 0.034$; Fig. 1D). CD8$^+$ T cells

were increased slightly in NCH and viral hepatitis including CH, PC, and LC compared with healthy controls. These results suggested that an immunoreaction had also occurred in nontumorous liver bearing HCC without viral hepatitis.

Clinicopathologic features of HCC and the prevalence of tumor-infiltrating Tregs and CD8⁺ T cells. We analyzed the correlation between clinicopathologic features of HCC and the prevalence of tumor-infiltrating Tregs or that of CD8⁺ T cells in HCC (Table 2A and B). Patients with HCC were divided into two groups either by the median value for the prevalence of tumor-infiltrating Tregs (29.0%) or by CD8⁺ T cells (51.5%). The high Treg group (n = 73) showed a significant correlation with high histologic grade (P = 0.021) and tended to show a lower number of infiltrating CD8⁺ T cells in HCC (P = 0.064) among the various clinicopathologic characteristics (Table 2A).

Prognostic significance of the prevalence of Tregs and CD8⁺ T cells in HCC. Overall and disease-free survival were analyzed in these patients. Of the 147 patients with HCC who underwent hepatic resection, 88 (59.9%) died. The overall 5-year survival and disease-free survival rates were 39.5% and 18.4%, respectively. The low-Treg group showed significantly better overall survival than the high-Treg group (log-rank test, P = 0.007; Fig. 1E). Mean overall survival was 60.3 (±33.8) months for the low-Treg group and 45.1 (±38.7) months for the high-Treg group. The low-Treg group also showed significantly better disease-free survival than the high-Treg group (log-rank test, P = 0.015; Fig. 1F). Mean disease-free survival was 36.2 (±31.7) months for the low-Treg group and 27.3 (±32.9) months for the high-Treg group. The 15 clinicopathologic factors listed in Table 3A and B were examined for their association with overall and disease-free survival after initial resection of the tumor. Univariate analysis of overall survival revealed that the following variables had a negative influence: Child-Pugh classification (B), TNM stage (III and IV), high serum α-fetoprotein (AFP; >27.1 IU/mL), presence of portal vein invasion (VP), presence of histologic intrahepatic metastatic foci (IM), and high prevalence of tumor-infiltrating Tregs (Table 3A). In multivariate Cox proportional hazard analysis for clinicopathologic variables and prevalence of tumor-infiltrating Tregs, the

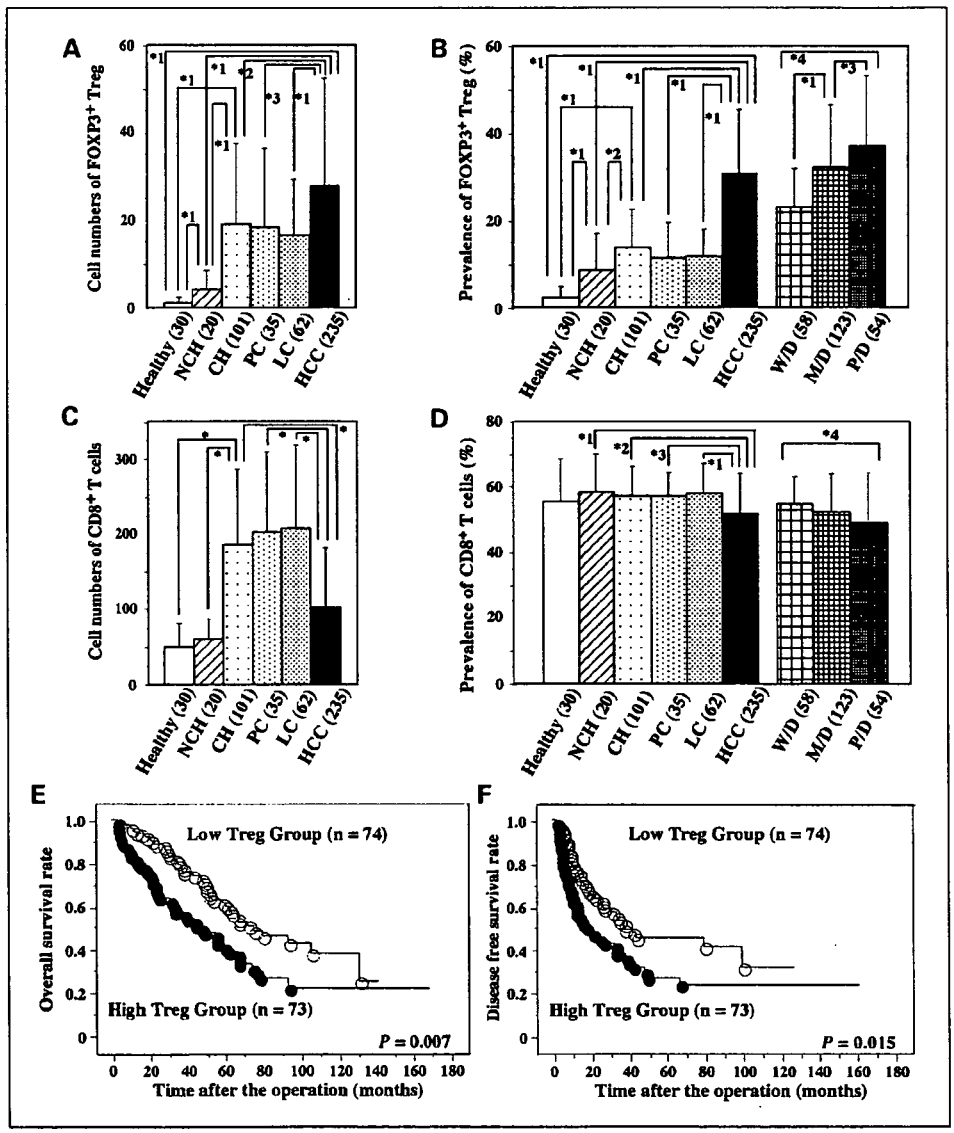

Fig. 1. Increased population of FOXP3⁺ Tregs and decreased population of CD8⁺ T cells in tumor stroma of HCC. *A* and *B*, absolute number of Tregs (*A*) and prevalence of Tregs (*B*) in HCC and nontumorous liver. Right column, the contents of HCC according to histologic grade (*B*). Number of cases tested in parentheses: *A*, *1, P < 0.001; *2, P = 0.002; *3, P = 0.023. *B*, *1, P < 0.001; *2, P = 0.021; *3: P = 0.044; *4, P < 0.001 (Kruskal-Wallis test); thin bars, SD. *C* and *D*, absolute number of CD8⁺ T cells (*C*) and prevalence of CD8⁺ T cells (*D*) in HCC and nontumorous liver. Right column, the contents of HCC according to histologic grade (*D*). Number of cases tested in parentheses: thin bars, SD. *C*, *, P < 0.001. *D*, *1, P = 0.025; *2, P < 0.001; *3, P = 0.015; *4, P < 0.001 (Kruskal-Wallis test). *E* and *F*, Kaplan-Meier survival curves of 147 patients with HCC. Overall survival curve (*E*) and disease-free survival curve (*F*) are shown. The prognosis was significantly worse in the high Treg prevalence group (*solid dots*, n = 73) than in the low Treg prevalence group [*white dots*, n = 74; log-rank test, P = 0.007 (*E*) and P = 0.015 (*F*)].

hazard ratio for poor prognosis was 1.640 for patients in the high-Treg group compared with patients in the low-Treg group ($P = 0.040$; Table 3A). Worse Child-Pugh classification and the presence of VP were also independent factors for overall patient survival. Univariate analysis for disease-free survival revealed that six variables negatively affected the survival rate and all of them were the same with the six variables of overall survival (Table 3B). In multivariate analysis for disease-free survival, two variables—the presence of IM and the high prevalence of Tregs infiltrating HCC—were significant factors. The hazard ratio for poor prognosis was 1.706 for patients in the high-Treg group compared with patients in the low-Treg group ($P = 0.024$; Table 3B). There was no significant difference in the overall survival rate or disease-free survival rate between the low and high $CD8^+$ T cell groups. These results indicated that the prevalence of tumor-infiltrating Tregs was an independent prognostic factor in patients with HCC, whereas the prevalence of tumor-infiltrating $CD8^+$ T cells was not.

Increased populations of Tregs among $CD4^+$ T cells in tumor stroma correspond to progression during multistage hepatocarcinogenesis. It was suggested that Tregs play important roles in the progression of HCC. Therefore, the prevalence of Tregs among $CD4^+$ T cells in the precursor lesions, AH ($n = 11$; Fig. 2E-H) and AAH ($n = 9$), and early HCC ($n = 68$; Fig. 2I-L), was analyzed during tumorigenesis of HCC. As shown in Fig. 3A, the prevalence of Tregs increased significantly in a stepwise manner during the progression of hepatocarcinogenesis (Kruskal-Wallis test, $P < 0.001$; viral hepatitis containing CH, PC, and LC versus precursor lesions containing AH and AAH, $P = 0.038$; precursor lesions versus early HCC, $P = 0.121$; early HCC versus advanced HCC, $P < 0.001$). These findings suggest that the prevalence of Tregs is closely correlated with the progression of multistage hepatocarcinogenesis. In contrast, the prevalence of $CD8^+$ T cells showed a clear, but not drastic, decrease during the progression of hepatocarcinogenesis (Kruskal-Wallis test, $P < 0.001$; Fig. 3B).

Table 2. Correlation between clinicopathologic findings and the prevalence of Tregs and $CD8^+$ T cells infiltrating HCC

(A) Correlation between clinicopathologic findings and the prevalence of Tregs infiltrating HCC

Variables	Prevalence of Tregs among $CD4^+$ T cells		
	High Treg	Low Treg	*P*
Age, y (mean ± SD)	62.6 ± 8.92	61.4 ± 10.4	0.444*
Gender (male/female)	59/14	54/20	0.259†
Viral infection			
HBV and/or HCV/(−)	66/7	69/5	0.531†
HBV(+)/(−)	27/7	29/5	0.525†
HCV(+)/(−)	45/7	43/5	0.640†
Nontumor liver (NCH/CH/PC/LC)	7/41/9/16	10/30/14/20	0.289†
Child-Pugh score (A/B/C)	68/5/0	68/6/0	0.772†
TNM stage (I/II/III/IV)	28/22/23/0	29/31/14/0	0.155†
Tumor size, mm (median, range)	40, 9-185	30, 6-150	0.113‡
Histologic grade (early HCC/WD HCC/MD HCC/PD HCC)	7/3/38/25	10/12/39/13	**0.021**†
AFP, ng/mL (median, range)	24.1 (1.8-27,170)	28.3 (1.0-25,000)	0.681‡
VP (presence/absence)	33/40	24/50	0.112†
IM (presence/absence)	20/53	13/61	0.152†
Number of $CD8^+$ T cells infiltrating tumor (median, range)	75 (12-405)	91 (9-435)	0.064‡

(B) Correlation between clinicopathologic findings and the prevalence of $CD8^+$ T cells infiltrating HCC

Variables	Prevalence of $CD8^+$ T cells in total T cells		
	High $CD8^+$ T cells	Low $CD8^+$ T cells	*P*
Age, y (mean ± SD)	63.6 ± 9.08	60.5 ± 10.0	0.051*
Gender (male/female)	51/23	62/12	**0.045**†
Viral infection			
HBV and/or HCV/(−)	69/4	66/8	0.238†
HBV(+)/(−)	30/4	26/8	0.203†
HCV(+)/(−)	42/4	46/8	0.348†
Nontumor liver (NCH/CH/PC/LC)	11/35/12/15	6/36/11/21	0.471†
Child-Pugh score (A/B/C)	67/6/0	69/5/0	0.736†
TNM stage (I/II/III/IV)	28/29/16/0	29/24/21/0	0.560†
Tumor size, mm (median, range)	40, 6-185	31, 10-150	0.075‡
Histologic grade (early HCC/WD HCC/MD HCC/PD HCC)	9/8/39/17	8/7/38/21	0.907†
AFP, ng/mL (median, range)	21.5 (1.0-27,170)	36.3 (1.8-17,430)	0.105‡
VP (presence/absence)	31/42	26/48	0.362†
IM (presence/absence)	18/55	15/59	0.524†

Abbreviations: MD, moderately differentiated; PD, poorly differentiated; WD, well differentiated.
*Student's *t* test.
†χ^2 test or Fisher exact test.
‡Mann-Whitney *U* test.